Expression Profiling of Immature Thymocytes Revealed a Novel Homeobox Gene That Regulates Double-Negative Thymocyte Development[1]

Masahito Kawazu,*† Go Yamamoto,* Mayumi Yoshimi,* Kazuki Yamamoto,* Takashi Asai,* Motoshi Ichikawa,* Sachiko Seo,* Masahiro Nakagawa,* Shigeru Chiba,† Mineo Kurokawa,* and Seishi Ogawa[2]*‡§¶

Intrathymic development of CD4/CD8 double-negative (DN) thymocytes can be tracked by well-defined chronological subsets of thymocytes, and is an ideal target of gene expression profiling analysis to clarify the genetic basis of mature T cell production, by which differentiation of immature thymocytes is investigated in terms of gene expression profiles. In this study, we show that development of murine DN thymocytes is predominantly regulated by largely repressive rather than inductive activities of transcriptions, where lineage-promiscuous gene expression in immature thymocytes is down-regulated during their differentiation. Functional mapping of genes showing common temporal expression profiles implicates previously uncharacterized gene regulations that may be relevant to early thymocytes development. A small minority of genes is transiently expressed in the CD44^{low}CD25^{+} subset of DN thymocytes, from which we identified a novel homeobox gene, *Duxl*, whose expression is up-regulated by Runx1. *Duxl* promotes the transition from CD44^{high}CD25^{+} to CD44^{low}CD25^{+} in DN thymocytes, while constitutive expression of *Duxl* inhibits expression of TCR β-chains and leads to impaired β selection and greatly reduced production of CD4/CD8 double-positive thymocytes, indicating its critical roles in DN thymocyte development. *The Journal of Immunology*, 2007, 179: 5335–5345.

Intrathymic development of thymocytes from their bone marrow progenitors is a critical process for the generation of mature T cells, through which the immature thymocyte progenitors, as identified by the absence of mature T cell markers (CD4/CD8 double-negative (DN)[3] T cells), differentiate into the CD4/CD8 double-positive (DP) cells, and finally produce CD4 or CD8 single-positive T cells. Although accounting for <5% of total thymocytes in mice, the DN thymocytes undergo a dynamic developmental process that is essential for the subsequent expansion into the DP population (1). Among these DN thymocytes, the earliest chronological subset (DN1) is recognized as a CD44^{high}C-Kit^{+}CD25^{-} population (2, 3). In the first wave of cytokine-dependent pre-T cell expansion, the DN1 cells begin to proliferate with concomitant up-regulation of CD25, giving rise to the DN2 population showing the CD44^{high}C-Kit^{+}CD25^{+} phenotype (4). The DN2 thymocytes then start to rearrange their *TCR* genes and down-regulate the CD44 expression to generate the CD44^{low}CD25^{+} DN3 subset (5). In the DN3 stage, thymocytes are subjected to a process called β selection and only those DN3 cells that have productively rearranged their *TCRβ* gene can survive and transit into CD44^{low}CD25^{-} DN4 thymocytes, followed by rapid expansion into the DP population (6–8).

During these early developmental processes, immature thymocyte progenitors lose their multilineage plasticity and exclusively commit to T cell differentiation. Under appropriate conditions, the DN1 population can generate multilineage hemopoietic components in vitro (9, 10), although there still remains some controversy with regard to their potential to B lineage differentiation (11). The potential of the multilineage commitment is more restricted in the DN2 stage, where cells can still give rise to NK cells and thymic dendritic cells, but no more B cells (10, 12–14), and after the DN2/DN3 transition and the succeeding β selection, thymocytes mostly lose their potential to multilineage plasticity and totally commit to T cell lineage (10).

Because these processes are thought to take place under tightly controlled gene expression, it is of particular importance to clarify the nature of this gene regulation and the key regulators involved in that regulation. To date, a number of molecules have been identified that regulate these developmental processes (15). *Notch1*-deficient thymocytes, for example, are not able to produce T cells but differentiate into B cells (16), while *pTα*, *TCRβ*, *Lck*, *SLP76*, and *Lat* are shown to be indispensable for β selection and their knockout mice show a severe maturational block at the DN3/DN4 transition (17). Similarly, the DN2/DN3 transition is completely blocked in *Runx1*-deficinet mice (18, 19) and also in double knockout mice of *pTα* and *common cytokine receptor γ-chain* genes (20). In contrast, it is well anticipated that these developmental processes in DN thymocytes should involve regulation of much

*Department of Hematology and Oncology, †Cell Therapy and Transplantation Medicine, and ‡Regeneration Medicine for Hematopoiesis; §21st Century Core of Excellence (COE) program, Graduate School of Medicine, University of Tokyo, University of Tokyo Hospital, Tokyo, Japan; and ¶Core Research for Evolutional Science and Technology, Japan Science and Technology Agency

Received for publication June 5, 2007. Accepted for publication July 23, 2007.

The costs of publication of this article were defrayed in part by the payment of page charges. This article must therefore be hereby marked *advertisement* in accordance with 18 U.S.C. Section 1734 solely to indicate this fact.

[1] This work was supported by Research on Measures for Intractable Diseases, Health and Labor, Sciences Research Grants, Ministry of Health, Labor and Welfare, Research on Health Sciences focusing on Drug Innovation, the Japan Health Sciences Foundation, and Core Research for Evolutional Science and Technology, Japan Science and Technology Agency.

[2] Address correspondence and reprint requests to Dr. Seishi Ogawa, Department of Regeneration Medicine for Hematopoiesis, Graduate School of Medicine, University of Tokyo, Bunkyo-ku, Tokyo, Japan. E-mail address: sogawa-tky@umin.ac.jp

[3] Abbreviations used in this paper: DN, double negative; DP, double positive; FL, fetal liver; rh, recombinant human; shRNA, small hairpin RNA; iTCRβ, intracellular TCRβ; qPCR, quantitative PCR; NGFRt, nerve growth factor receptor; OP9-DL1, OP9-delta-like-1.

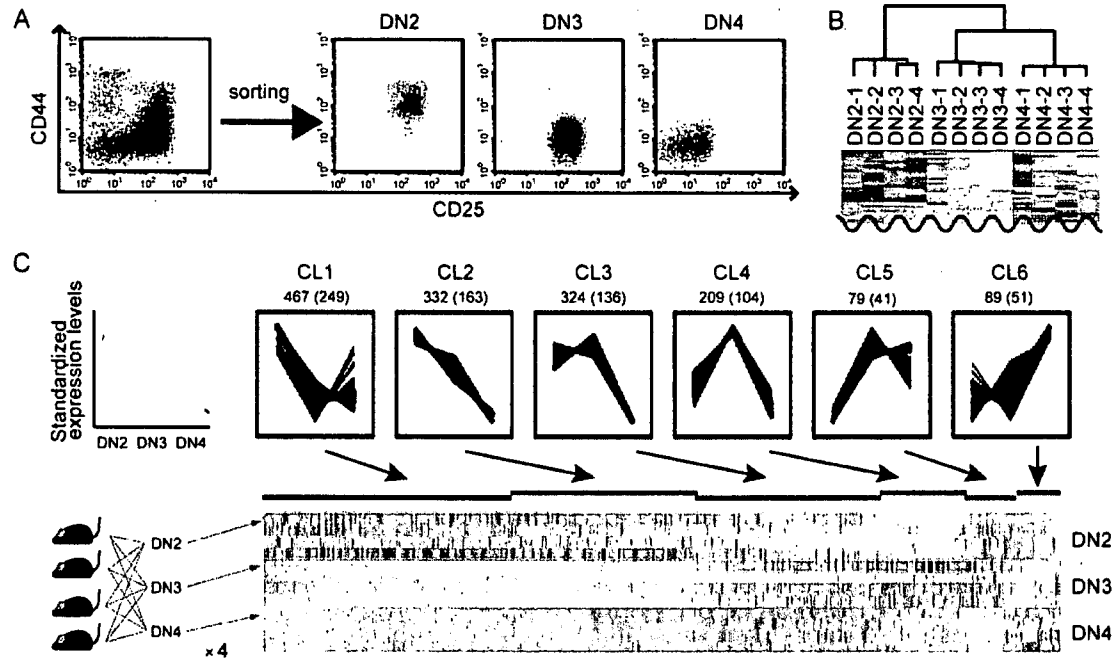

FIGURE 1. Microarray analysis and clustering of genes differentially expressed during early thymocyte development. *A*, DN2, DN3, and DN4 thymocytes from four C57BL/6 mice were FACS sorted and subjected to microarray analysis of gene expression profiles. *B*, Hierarchical clustering of 12 microarray data obtained from four independent experiments. Only branch portion is presented. *C*, One thousand five hundred differentially expressed genes were grouped into six clusters showing discrete temporal expression profiles by K-means clustering methods (*upper panels*), which are also presented in heat map (*lower panel*). The expression values for a gene across all samples were standardized to have a mean 0 and SD 1. Standardized expression levels of genes are indicated in graphs (*upper panels*) and in heat map (*lower panel*). Vertical scale of the graphs is from −1.5 to +1.5. Each column of heat map represents a gene and each row represents a sample. Red indicates high expression and blue low expression. The numbers of genes within clusters are indicated along with those for which human counterparts were identified (in the parentheses).

larger numbers of genes than those related to these known molecules. To understand the molecular mechanisms of DN thymocyte development, it may be also of use to clarify how these developmental processes are regulated in terms of their entire gene expression, to which cell differentiation is ultimately ascribed.

In the current study, we approached this issue by investigating gene expression profiles in discrete subsets of DN thymocytes under development in which DN2, DN3, and DN4 thymocytes were sorted and subjected to expression profiling analysis with high-density oligonucleotide microarrays. Clustering of differentially expressed genes among these DN thymocyte subsets demonstrated that during DN development, regulation of gene expression is predominantly repressive rather than inductive, in which multiple lineage-affiliated genes expressed in immature thymocytes are down-regulated during the course of DN thymocyte development. Functional mapping of clustered genes also revealed a possible involvement of previously uncharacterized functional gene regulations in thymocyte development. Finally, we identified a novel homeobox gene (*Duxl*), transiently expressed in DN3 thymocytes. We showed that *Duxl* is induced by Runx1 and regulates DN thymocyte development by promoting the DN2/DN3 transition, while deregulated expression of *Duxl* resulted in impaired β selection and severely compromised production of DP thymocytes, indicating its critical roles in DN thymocyte production.

Materials and Methods

Cell sorting and RNA extraction

All Abs used for cell sorting were purchased from BD Pharmingen. Thymocytes were harvested from 5- to 6-wk-old female C57BL/6 mice. Four independent cell sortings were performed and four mice were sacrificed for each experiment. Before cell sorting, $CD4^+$ cells and $CD8^+$ cells were depleted using the MACS LD system (Miltenyi Biotec). The remaining fraction was stained with anti-CD44 and anti-CD25 Abs conjugated to FITC or PerCP-Cy5.5, respectively, and also with PE-conjugated Abs to CD4, CD8, CD3, NK1.1, and TCR$\gamma\delta$ and sorted using a FACSAria cell sorter (BD Biosciences). DN2, DN3, and DN4 subsets were identified as $FITC^+PE^-PerCP^-Cy5.5^+$, $FITC^-PE^-PerCP^-Cy5.5^+$, and $FITC^-PE^-PerCP^-Cy5.5^-$ populations, respectively. For expression analysis of various hemopoietic lineages, mononuclear cells were separated from a single-cell suspension of bone marrow of 5- to 6-wk-old female C57BL/6 mice by centrifugation on a Histopaque-1083 (Sigma-Aldrich). $c\text{-}kit^+$ cells were obtained by positive selection for the c-kit Ag with MACS magnetic beads. The remaining fraction was stained with FITC-conjugated Ab to Ter119, PerCP-conjugated Ab to B220, and PE-conjugated Abs to Mac1, and $Ter119^+$ fraction, $B220^+$ fraction, and $Mac1^+$ fraction were sorted. B220+ splenocytes and CD3+ splenocytes were collected by positive selection of splenocytes for the B220 Ag or CD3 Ag with MACS magnetic beads. RNA was extracted from sorted cells using an RNeasy Mini kit (Qiagen) according to the manufacturer's instruction.

Microarray experiments

Biotin-labeled cRNA probes were prepared using a Two-Cycle cDNA Synthesis Kit (Affymetrix). Following fragmentation, biotin-labeled cRNA was hybridized to the Mouse Genome 430 2.0 Array (Affymetrix) for 16 h at 45°C as recommended by the manufacturer. Washing was performed using an automated fluidics workstation, and the array was immediately scanned with GeneChip Scanner 3000 7G. Expression data were extracted from image files produced on Affymetrix GeneChip Operating software 1.0 (GCOS). The absolute detection call (present, absent, or marginal) for each probe set was determined on GCOS. Normalization and expression value calculation were performed using a DNA-Chip Analyzer (www.dchip.org) (21). The invariant set normalization method (22) was used to normalize arrays at probe cell level to make them comparable and the model-based method (22) was used for computing expression values. These expression levels were attached with SEs as measurement accuracy, which were subsequently used to compute 90% confidence intervals of fold changes in two group comparisons (22). The lower confidence bounds of fold changes

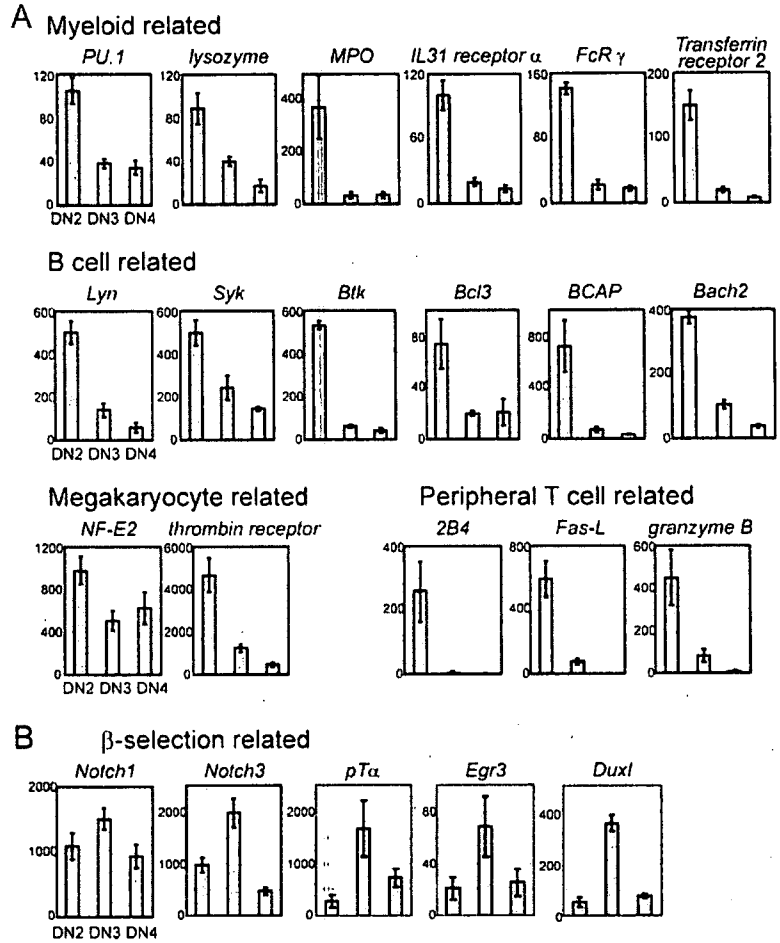

FIGURE 2. Expression patterns of lineage-affiliated genes and genes involved in β selection. Signal intensities on microarray for representative genes affiliated with various hemopoietic lineages are shown in *A* and for those relevant to β selection in *B* by their mean values (±SD), where the outlier data were excluded from the calculation. Expression data for *Duxl* are also presented in *B*.

were conservative estimate of the real fold changes. Differentially expressed probe sets were identified as those sets whose mean signals showed >1.5-fold difference between DN2 and DN3 and DN3 and DN4. The probability of false discoveries with this threshold was calculated by random permutations as described previously (23). Raw microarray data can be found at http://www.ncbi.nlm.nih.gov/geo/, GEO accession no. GSE7784.

Clustering and pathway analysis

One thousand five hundred differentially expressed genes that were identified as described above were clustered using a K-means (24) server on Gene Expression Pattern Analysis Suite (http://gepas.bioinfo.cnio.es/) (25, 26). Molecular network of each cluster was analyzed by KeyMolnet software, which was developed by the Institute of Medicinal Molecular Design, Inc. (IMMD) (27). Known molecular data were curated by IMMD and the obtained gene list of each cluster was combined with this software and shown as molecular networks. Significance of a determined pathway to obtained networks was determined. To ascertain whether any molecular pathways determined by IMMD annotate a relation between molecules in the networks at a frequency greater than that would be expected by chance, this software calculates a p value using the hypergeometric distribution as described previously (28).

Cloning of Duxl cDNA and construction of retrovirus plasmid

cDNAs of Duxl and FLAG-tagged Duxl having *Not*I and *Xho*I sites on their 5′ and 3′ terminus, respectively, were PCR amplified from template cDNA prepared from total thymic RNA using TaKaRa LA *Taq* (Takara Bio) with the following sets of primers: 5′-AAAAGCGGCCGCATCGA TACCATGGAGCTGAGCTGCAGTACT-3′ (for Duxl sense), 5′-AAAA GCGGCCGCATCGATACCATGGACTACAAGGACGACGATGACAA GATGGAGCTGAGCTGCAGTACT-3′ (for FLAG-tagged Duxl sense), and 5′-AAAACTCGAGCTACGGAGTTTGGTGTGCTT-3′ (for the common antisense for both). Each PCR product was digested with *Not*I and *Xho*I and cloned into the *Not*I-*Xho*I site located at the 5′ upstream of IRES-GFP or IRES-NGFRt of the pGCDNsam (a gift from Dr. H. Nakauchi, University of Tokyo, Tokyo, Japan) retrovirus vector. Nucleotide sequences of these plasmids were confirmed by resequencing. Retrovirus was prepared by transfecting the PlatE (a gift from Dr. T. Kitamura, University of Tokyo) cell line with each construct.

Quantitative PCR analysis

Total cellular RNA was converted into cDNAs by reverse transcriptase (Superscript III; Invitrogen Life Technologies) with random primers. cDNAs were amplified in triplicate for 40 cycles at 95°C for 15 s and 60°C for 60 s using an Applied Biosystems PRISM 7000 Sequence Detection System according to the manufacturer's instructions. Predesigned TaqMan primer and probe sets for 1110051B16Rik (Mm00841823_m1; Applied Biosystems) (see Fig. 4), for PU.1 (Mm00488140_m1), and for 18S rRNA (no. 4308329; Applied Biosystems) were used for the assay. PCR amplification of GAPDH, 1110051B16Rik (see Fig. 5*B*) and Rag1 was performed using Platinum SYBR Green qPCR SuperMix-UDG with ROX (Invitrogen Life Technologies) and the following primer sequences: GAPDH (forward, 5′-GAATCTACTGGAGTCTTCACC-3′; reverse, 5′-GTCATGAGCCCTTCCACGATGC-3′), 1110051B16Rik (forward, 5′-GGGAAAACTGGCTCAACAA-3′; reverse, 5′-GTGTTCTGTCCTGG GTCTGG-3′), Rag1 (forward, 5′-CTGAAGCTCAGGGTAGACGG-3′; reverse, 5′-CAACCAAGCTGCAGACATTC-3′). Significant PCR fluorescent signals were normalized for each sample to a PCR fluorescent signal obtained using GAPDH or 18S rRNA as control.

Coculture of fetal liver (FL) cells with OP9-delta-like-1 (OP9-DL1) stromal cells

OP9-DL1 is a bone marrow stromal cell line that expresses a Notch ligand, Delta-like 1, and supports development of DP thymocytes from FL-derived hemopoietic progenitors (29) and was provided by Dr. J. C. Zúñiga-Pflücker (University of Toronto, Toronto, Canada). In our OP9-DL1 assay, FL cells were harvested from E14.5 embryos and cultured on OP9-DL1 cells

in combination with retroviral gene transfer as previously described (19). Briefly, mononuclear cells were separated from FL cells of C57BL/6 mice. In brief, 5×10^4 mononuclear cells were cultured on confluent OP9-DL1 cells in flat-bottom 24-well culture plates with 500 ml of MEM (Invitrogen Life Technologies) supplemented with 20% FCS, penicillin/streptomycin, and 5 ng/ml recombinant human (rh) IL-7 (Techne Laboratories). After 5 or 6 days of culture, 5×10^4 cells were passed onto newly prepared OP9-DL1 cells in the presence of 5 ng/ml rhIL-7, and retrovirus infection was performed using polybrene (final concentration, 8 mg/ml), followed by another 5 or 6 days of culture. In brief, 5×10^4 cells were again passed onto newly prepared OP9-DL1 cells and cultured for another 5 or 6 days, but in rhIL-7-free culture medium.

PCR for TCRβ rearrangement

PCR for TCRβ rearrangements was performed as described elsewhere (30) on DNA isolated from FL cells cultured on OP9-DL1 using the following primers: Dβ2, GTAGGCACCTGTGGGGAAGAAACT; Jβ2, TGAGAG CTGTCTCCTACTATCGATT; and Vβ5.1, GTCCAACAGTTTGATGAC TATCAC. After 40 cycles of amplification (10 s at 98°C, 2 min at 68°C), PCR products were separated on a 4% agarose gel.

RNA interference

The vector backbone was RNAi-Ready pSIREN-RetroQ-ZsGreen (BD Clontech). The RNA interference target sequences were GGAGCAG GATAAACCTAGA (sequence 1), GACTGATATTCTAATTGAA (sequence 2), and GTTCCAGACTGATATTCTA (sequence 3). The small hairpin RNA (shRNA) were designed by a shRNA design algorithm, which was developed by Dr. M. Miyagishi (31). Oligonucleotides used for construction were GATCCGGGGTAGGATAAACTTAGAACGTGTGCTGT CCGTTCTAGGTTTATCCTGCTCCTTTTTACGCGTG (oligonucleotide 1, sense), AATTCACGCGTAAAAAGGAGCAGGATAAACCTAGAAC GGACAGCACACGTTCTAAGTTTATCCTACCCCG (oligonucleotide 1, antisense), GATCCGATTGATGTTCTAGTTGAAACGTGTGCTGTC CGTTTCAATTAGAATATCAGTCTTTTTACGCGTG (oligonucleotide 2, sense), AATTCACGCGTAAAAAGACTGATATTCTAATTGAAACG GACAGCACACGTTTCAACTAGAACATCAATCG (oligonucleotide 2, antisense), GATCCGTTTCAGATTGATGTTCTAACGTGTGCTGTCCG TTAGAATATCAGTCTGGAACTTTTTACGCGTG (oligonucleotide 3, sense), and AATTCACGCGTAAAAAGTTCCAGACTGATATTCTAAC GGACAGCACACGTTAGAACATCAATCTGAAACG (oligonucleotide 3, antisense). Retrovirus was prepared by transfecting the PlatE cell line with the knockdown vectors.

Results

Clustering of differentially expressed genes during DN thymocyte development

The DN2, DN3, and DN4 populations were FACS sorted from DN thymocytes harvested from four C57BL/6 mice and analyzed by an Affymetrix Mouse Genome 430 2.0 Array for gene expression (Fig. 1*A*). Four independent experiments were performed using 16 mice. After normalizing the array signals using an invariant gene set (22), we extracted differentially expressed probe sets whose signals showed ≥1.5-fold difference between DN2 and DN3 or between DN3 and DN4. With this threshold, 1,901 probe sets (or 1,500 nonredundant genes) were extracted as "differentially expressed" from a total of 27,330 probes (16,131 genes) expressed in either of the three DN subsets, with a false discovery rate of 0.007 as determined by random permutation tests (23). In hierarchical clustering, the four independent array data sets for each subset were correctly clustered into the same clusters, validating the reproducibility across the experiments (Fig. 1*B*). In contrast, the K-means clustering of the 1,500 differentially expressed genes identified six clusters, CL1–CL6, showing discrete temporal expression profiles: genes expressed higher in DN2 and down-regulated in DN3 (CL1), those expressed higher in DN2 and gradually down-regulated in DN3 and DN4 (CL2), those expressed in DN2 and DN3 but down-regulated in DN4 (CL3), those only transiently expressed in DN3 (CL4), those expressed both in DN3 and DN4 (CL5), and those showing low expression in DN2 and DN3 and up-regulated in DN4 (CL6) (Fig. 1*C*). The lists of genes in these clusters were presented in supplementary Table S1, a–f.[4]

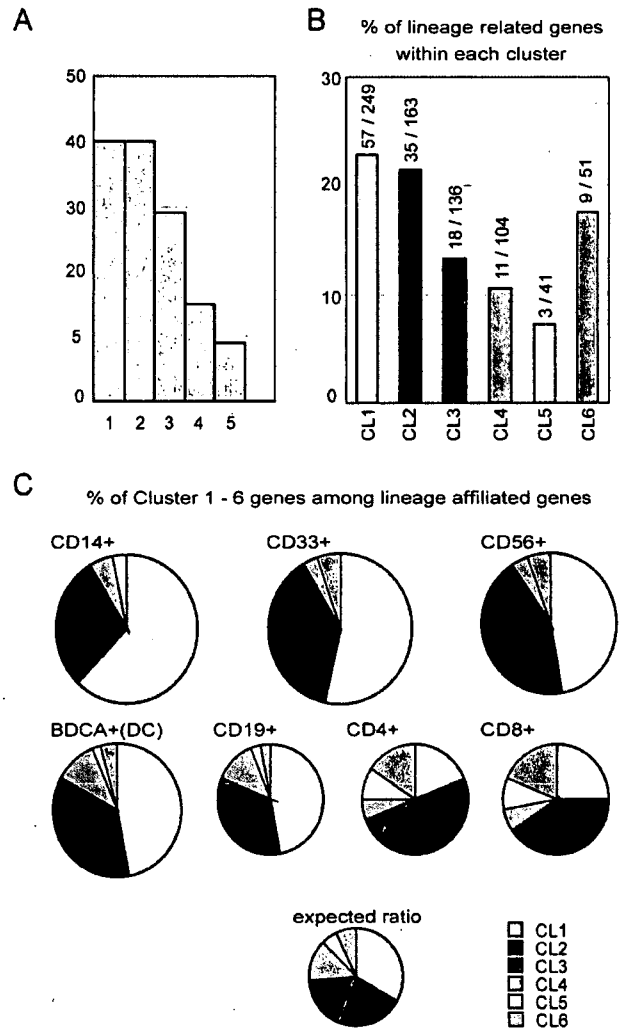

FIGURE 3. Temporal expression profiles of hemopoietic lineage-affiliated genes. *A*, Histogram of the number of lineage-affiliated genes with regard to the number of lineages to which each gene is assigned. *B*, Percentages of lineage-affiliated genes within each cluster showing discrete temporal expression profiles. Absolute numbers of lineage-affiliated genes and all genes in each cluster are shown above the bar. *C*, Number and composition of different lineage-affiliated genes with regard to clusters. Area of each circular graph represents the number of genes affiliated with each lineage.

Predominantly repressive gene regulation in DN thymocytes and their lineage-promiscuous gene expression

With regard to the temporal profiles of gene expression in DN thymocytes, our first note is that 1123 (74.9%) of the 1500 differentially expressed genes are initially expressed in DN2 but eventually down-regulated during the course of DN thymocyte development (CL1–3), while only 79 (5.27%) and 89 (5.93%) genes are up-regulated in DN3 and DN4 (CL5 and CL6), respectively (Fig. 1*C*). The other set of genes (CL4) are transiently expressed in DN3 but have low expression in DN2 and DN4. Thus, gene regulation during DN thymocyte development is largely repressive rather than inductive. Our next note was that these down-regulated genes

[4] The online version of this article contains supplemental material.

Table I. *Significantly relevant pathways in each cluster*

Rank	Name	p
CL1		
1	Ets (Spi subfamily) regulation	3.84×10^{-9}
2	IL-4 signaling	1.35×10^{-8}
3	IgG signaling	1.39×10^{-4}
4	Integrin signaling	6.94×10^{-4}
5	c-kit signaling	1.47×10^{-3}
6	G protein (G12/13) signaling	1.55×10^{-3}
7	Ets (TCF subfamily) regulation	3.11×10^{-3}
8	Rho family signaling	8.30×10^{-3}
9	CD44 signaling	8.60×10^{-3}
CL2		
1	RUNX regulation	2.19×10^{-7}
2	Endoplasmic reticulum regulation	9.72×10^{-5}
3	Platelet-derived growth factor signaling	4.94×10^{-4}
4	Prolactin signaling	7.09×10^{-4}
5	PI3K signaling	1.23×10^{-3}
6	γ-Aminobutyric acid signaling	1.23×10^{-3}
7	IL-2 signaling	1.78×10^{-3}
8	CCR10 signaling	4.66×10^{-3}
9	G protein (Gq/11) signaling	5.87×10^{-3}
10	Human growth factor signaling	9.55×10^{-3}
CL3		
1	NFAT regulation	9.67×10^{-8}
2	AP-1 regulation	3.12×10^{-5}
3	Caspase signaling	3.59×10^{-3}
4	PPARα regulation	5.24×10^{-3}
CL4		
1	TCRαβ signaling	2.35×10^{-6}
2	Ets (Ets family) regulation	1.40×10^{-5}
3	Integrin signaling	1.87×10^{-3}
4	NF-κB regulation	7.58×10^{-3}
5	Notch signaling	8.23×10^{-3}
CL5 and 6		
1	Integrin signaling	1.67×10^{-6}
2	TCRαβ signaling	7.23×10^{-6}
3	Ets (Ets family) regulation	3.17×10^{-5}
4	RB/E2F regulation	2.64×10^{-4}
5	TCF regulation	4.53×10^{-4}

contain a variety of genes whose expression is relatively characteristic to one or more hemopoietic lineages (lineage affiliated), including *NF-E2* and *thrombin receptor* (megakaryocytes), *PU.1*, *lysozyme*, and *myeloperoxidase* (myeloid lineages), *Lyn*, *Syk*, *Btk*, *Bcl3*, *BCAP*, and *Bach2* (B cells), and *2B4*, *Fas ligand*, and *granzyme B* (mature T cells) (Fig. 2*A*). This suggested that "promiscuous" expression of multiple lineage-affiliated genes in early thymocyte progenitors and their repression during the course of their commitment to mature T cells could be one of the characteristics of immature thymocytes. To confirm this in more detail, we identified those genes whose expression was thought to characterize a variety of mature hemopoietic lineages and tracked their expression levels during the course of DN thymocyte development. Because no comprehensive gene expression database was available for mice, we did this using a human tissue expression database at the Genomics Institute of the Novartis Research Foundation web site (http://symatlas.gnf.org/SymAtlas/) (32) by translating mouse genes into their human counterparts. A gene is considered to be affiliated with a lineage if its human counterpart shows >10 times higher expression in that lineage than their median expression among 79 different tissues. Among the 1500 differentially expressed genes, the human counterparts were uniquely identified for 744 (49.6%) genes (Fig. 1*C*), of which 133 (17.9%) satisfied the above criteria for being affiliated with one or more hemopoietic cell lineages (Fig. 3*A*), and lists of genes affiliated with respective lineages are presented in supplementary Table S2, a–g.[4] Among the 133 lineage-affiliated genes, 110 (83%) are expressed in DN2 and down-regulated during the course of the DN thymocyte development (CL1–CL3), accounting for 20% of 548 down-regulated genes assigned to CL1–3 (Fig. 3*B*). More genes are rapidly down-regulated during the DN2/DN3 transition (CL1), whereas as indicated from the relatively high CL3 component, down-regulation of genes affiliated with NK cells seems to occur more slowly (Fig. 3*C*). Although most of these down-regulated genes are affiliated with lineages other than T cells, many T cell-affiliated genes are also prematurely expressed in immature thymocytes and undergo down-regulation before they are definitely expressed later in thymocyte maturation (Figs. 2*A* and 3*C*). Only 12 (9%) lineage-affiliated genes were newly up-regulated until the DN4 stages and mostly related to T cells (Fig. 3, *B* and *C*). Note that our criteria for lineage relatedness may be too conservative, since many of genes presumed to be specific to mature T cells, such as *2B4*, *Fas ligand*, and *granzyme B*, were not extracted as T cell-related genes.

Pathway analysis of gene clusters during DN thymocytes development

The functional features of genes showing discrete expressional time courses are of interest to understand the regulation of DN development. To address this, we statistically explored possible functional links among genes within each cluster by evaluating a probability that a given set of genes on the known functional pathway was grouped together by chance within that cluster, showing a similar temporal expression profile using KeyMolnet software

Table II. *List of genes in CL4 with presumed DNA-binding capacity*

Entrez Gene Identification	Gene Title	GO Molecular Function Description
26972	Sporulation protein, meiosis-specific, SPO11 homolog (*Saccharomyces cerevisiae*)	DNA binding, DNA topoisomerase (ATP-hydrolyzing) activity, ATP binding, hydrolase activity
18131	Notch gene homolog 3 (*Drosophila*)	DNA binding, transcription factor activity, receptor activity, calcium ion binding, protein binding
72693	Zinc finger, CCHC domain containing 12	Nucleic acid binding, zinc ion binding, metal ion binding
278672	RIKEN cDNA 1110051B16 gene	DNA binding, transcription factor activity, sequence-specific DNA binding
13655	Early growth response 3	Nucleic acid binding, DNA binding, zinc ion binding, metal ion binding
210104	cDNA sequence BC043301	Zinc ion binding, metal ion binding, nucleic acid binding
320790	Chromodomain helicase DNA binding protein 7	—
67344	Tctex1 domain containing 1	—
15463	HIV-1 Rev-binding protein	DNA binding, zinc ion binding, metal ion binding
272382	SpiB transcription factor (Spi1/PU.1 related)	DNA binding, transcription factor activity, sequence-specific DNA binding, transcription factor activity

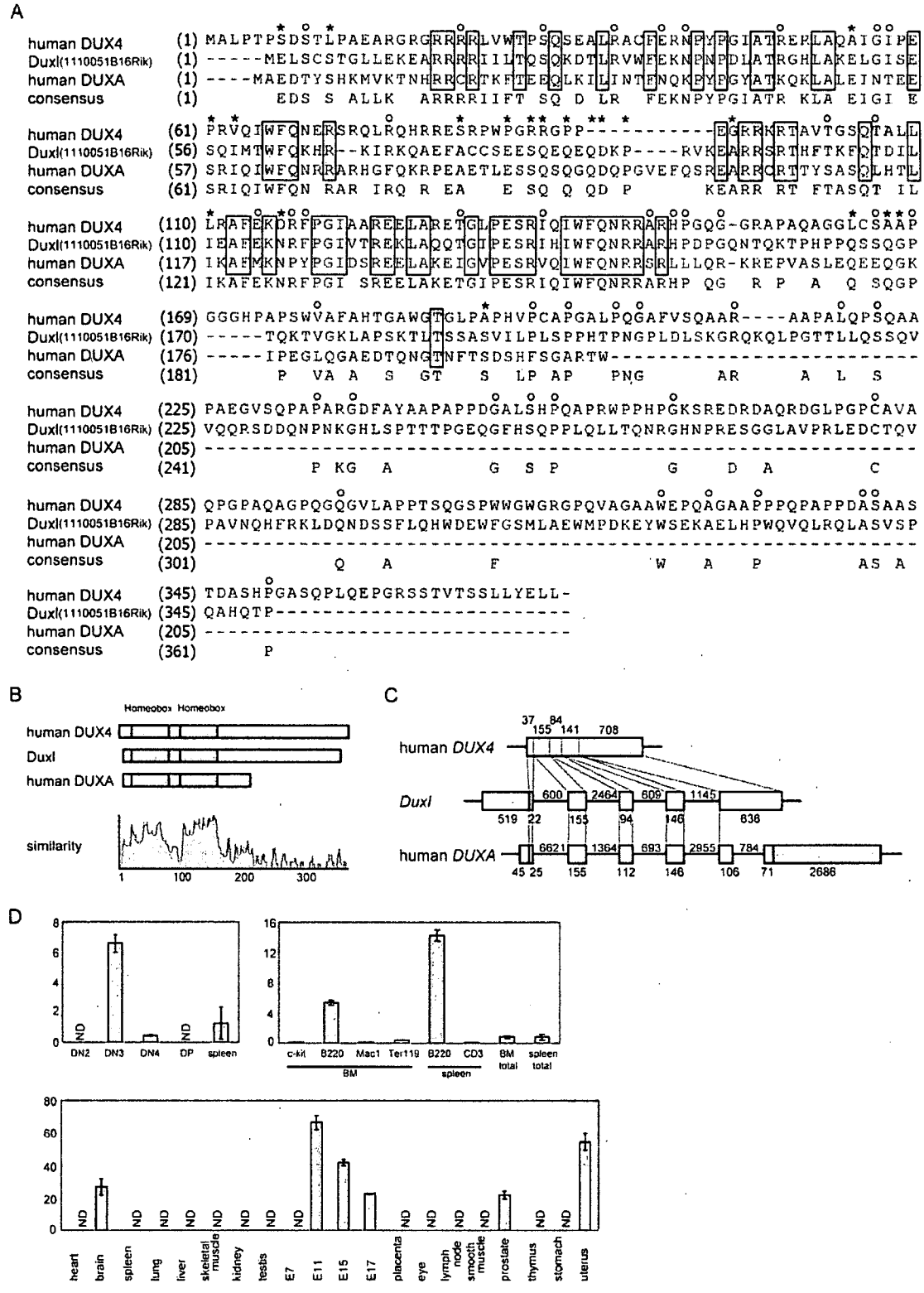

FIGURE 4. Structure of Duxl and similarity to its candidate orthologs. *A*, Homology of Duxl to its putative human orthologs (DUXA and DUX4) in amino acid sequences in which boxes indicate the identical amino acids among the three genes, asterisks indicate the common amino acids between Duxl and DUXA, and open circles indicate the common amino acids between Duxl and DUX4. *B*, Structure of predicted Duxl protein with its similarity to DUXA and DUX4. *C*, Gene structures of *Duxl* in mouse and *DUXA* and *DUX4* in humans. *D*, Distribution of *Duxl* expression in various tissues and cell lineages as determined by qPCR. The amount of transcript of *Duxl* was normalized to the amount of 18S rRNA in each tissue/population and is shown relative to levels in the total splenocytes in the *upper right panel*. Data shown are the average ± SD from triplicate samples.

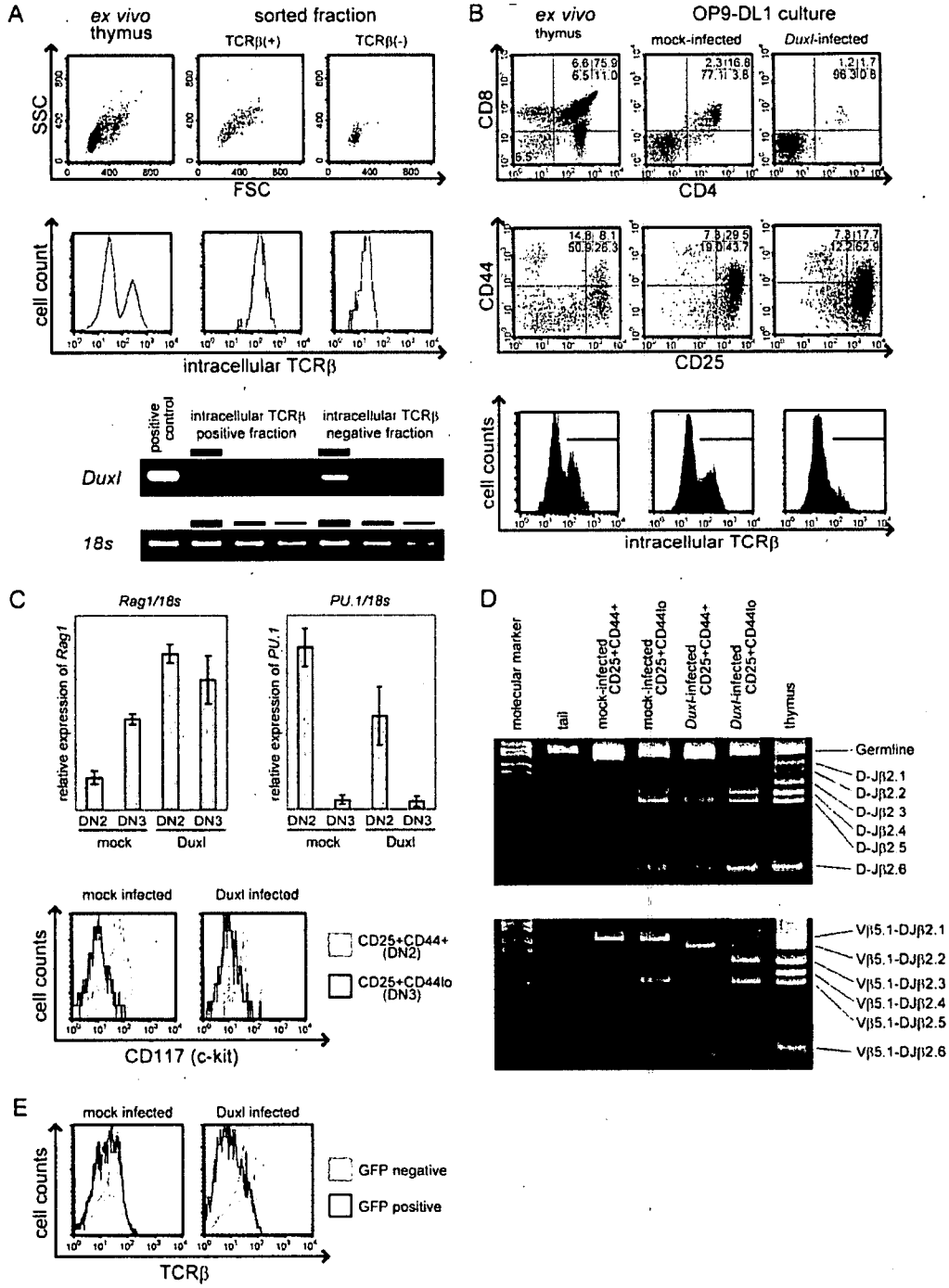

FIGURE 5. Effect of *Duxl* transduction on thymocyte development in OP9-DL culture. *A*, DN3 cells from normal mice were FACS sorted according to the expression of iTCRβ chain (*upper two panels*) and expression of *Duxl* in iTCRβ$^+$ and iTCRβ$^-$ cells was examined by qPCR analysis. Resultant PCR products were electrophoresed on 4% agarose gel (*lower two panels*). *B*, *Duxl* was transduced into FL cells and the development into thymocytes was examined by FACS analysis for their expression of CD4/CD8 (*upper panels*), CD25/CD44 (*middle panels*), and iTCRβ chains (*bottom panels*) in ex vivo thymus (*left*), mock-infected cultured FL cells (*middle*), and *Duxl*-transduced cultured FL cells (*right*). *C*, Expression levels of *Rag1* and *PU.1* were examined by qPCR using RNA isolated from the sorted GFP$^+$CD25$^+$CD44$^+$ fraction and GFP$^+$CD25$^+$CD44^{low} fraction of mock- or *Duxl*-transduced FL cells cultured on OP9-DL1 (*upper panels*). The amount of transcript of *Rag1* and *PU.1* was normalized to the amount of 18S rRNA in each population and is shown as relative values. Data shown are the average ± SD from triplicate samples. Expression of CD117 was analyzed with FACS (*lower panels*). *D*, TCRβ rearrangement status was analyzed by PCR using DNA isolated from the sorted GFP$^+$CD25$^+$CD44$^+$ fraction and GFP$^+$CD25$^+$CD44^{low} fraction of mock- or *Duxl*-transduced FL cells cultured on OP9-DL1. *E*, *Duxl* was overexpressed in FL cells or AKR1 cells using retrovirus vector, and the expression levels of TCRβ in the GFP$^+$ fraction were examined by FACS.

(IMMD) (27). Because of the small numbers of genes within the clusters CL5 and CL6, both clusters were analyzed after being combined together. In this pathway analysis, several sets of functionally related genes or pathways were extracted from each cluster. Table I shows a list of pathways extracted in high significance values ($p < 0.01$). For examples, genes involved in c-kit signaling

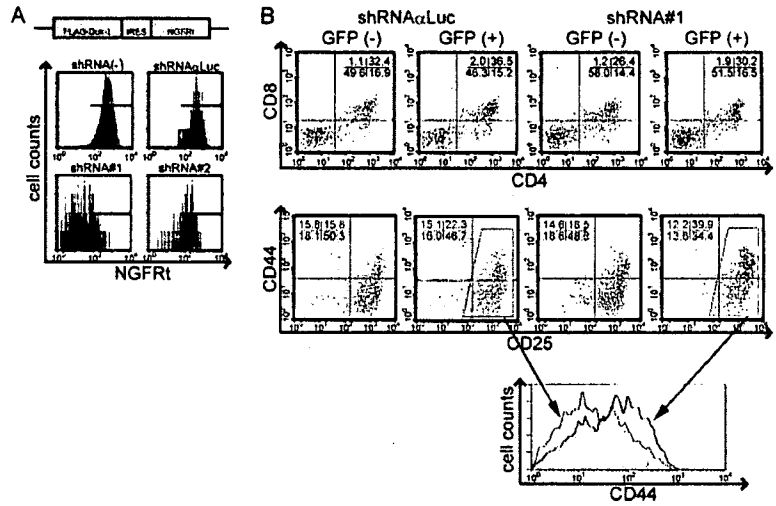

FIGURE 6. Effect of *Duxl* knockdown on expression levels of CD44. *A*, NIH3T3 cells stably expressing FLAG-Duxl-IRES-NGFRt (*upper left*) were infected with retroviruses encoding shRNA directed against a luciferase sequence (αLuc; *upper right*) or shRNA against a DuxL sequence #1 (*lower left*) and sequence #2 (*lower right*). Transduction of shRNA was tracked by GFP. NGFRt expression on GFP$^+$ cells was analyzed by flow cytometry. *B*, FL cells infected with Luc-shRNA retroviruses (αLuc) or Duxl-shRNA retroviruses (sequence #1) were cultured on OP9-DL1 cells and expression of CD4/CD8 (*upper panels*) and CD25/CD44 (*lower panels*) was analyzed after 17 days. Dot plots are gated on GFP$^-$CD4$^-$CD8$^-$ cells or GFP$^+$CD4$^-$CD8$^-$ cells.

(p = 0.00147) and CD44 signaling (p = 0.0086) were extracted from the CL1 cluster, reflecting the fact that c-*kit* and *CD44* are down-regulated in DN3 and also indicating that the pathways extracted from CL1 are expected to be inactivated in DN3. Other pathways that are known to undergo dynamic regulations during DN thymocyte development were also extracted from different clusters, including the Runx1 pathway from CL2 (gradually down-regulated), NFAT and AP-1 pathways from CL3 (down-regulated in DN4), TCR$\alpha\beta$, NF-κB, and Notch pathways from CL4 (transiently activated in DN3), and Ets and TCR$\alpha\beta$ pathways from CL5/CL6 (up-regulated in DN3 or DN4). The other pathways that were extracted with high significance values but have not been previously implicated in T cell development include those related to platelet-derived growth factor, γ-aminobutyric acid, and peroxisome proliferator-activated receptor α.

Expression and structure of 110051B16Rik *or* Duxl *gene*

In view of clarifying gene regulations that operate during thymocyte development, of particular interest are genes included in CL4, because they show a unique temporal expression profile of transient induction or up-regulation in DN3 and contain key genes for the thymocyte development or β selection, including *pre-TCRα*, *SpiB*, *Egr3*, and *Notch3* (33–37) (Fig. 2*B*). Especially, we were interested in genes that were thought to be involved in transcriptional regulations (Table II). Among these genes, we focused on a gene, *1110051B16Rik*, which encodes a putative transcription factor with unknown functions (Table II and Fig. 4*A*). It has an open reading frame of 1050 nt and the predicted protein shares structural features and sequence similarities with the families of double homeobox proteins that are thought to have rapidly diverged during evolution (Fig. 4*B*) (38). Although currently no definite human ortholog is uniquely identified due to incomplete sequence homology to human sequences, it shows the highest similarity with human DUXA or DUX4 in their amino acids sequence and gene structure with DUXA (Fig. 4, *B* and *C*), and thus, was named as *Duxl* (*Dux* in lymphoid lineage). In hemopoietic compartments, expression of *Duxl* is largely restricted to DN3 thymocytes and B220-positive B cells in bone marrow and spleen, implicating their functional roles in both subsets of lymphocytes, although it is also expressed in embryos from mid to late gestation, as well as in other non-hemopoietic adult organs, including brain, prostate, and uterus (Fig. 4*D*).

Function of Duxl *in thymocyte development*

To get an insight into the role of *Duxl* in thymocyte development, we first examined its expression among the subpopulations of DN3 thymocytes by FACS sorting DN3 cells into two populations according to their expression of intracellular TCRβ (iTCRβ) chains (Fig. 5*A*, *upper panel*) (8, 39). In quantitative PCR (qPCR) analysis, *Duxl* transcripts were detected in the iTCRβ$^-$ fraction (DN3a) but not in the iTCRβ$^+$ fraction (DN3b), indicating that the *Duxl* expression is largely restricted to the DN3a fraction (Fig. 5*A*, *lower panel*).

To explore the effect of constitutively expressed *Duxl* on DN thymocyte differentiation, we transduced the *Duxl* cDNA into mouse FL cells using a bicistronic retrovirus vector with a marker GFP cDNA in the second cistron, and the *Duxl*-transduced FL cells were then assayed on the OP9-Delta-1 (OP9-DL1) culture system that can mimic intrathymic development of DP thymocytes from the FL hemopoietic progenitors (29). As previously described, the mock-infected FL cells generated substantial numbers of GFP$^+$ DP thymocytes after 15 days of culture on OP9-DL1 (Fig. 5*B*, *upper central panel*) (19). In contrast, the number of GFP$^+$ DP cells was dramatically reduced in the culture from the *Duxl*-transduced FL cells (Fig. 5*B*, *upper right panel*). Although the total cell numbers were not significantly different between both cultures, the GFP$^+$ cells from the *Duxl*-transduced culture generated an increased proportion of the CD25$^+$CD44^{low} cells, compared with mock-infected cells (Fig. 5*B*, *middle panels*) that produced a similar proportion of CD25$^+$CD44^{low} cells as GFP$^-$ cells (data not shown). The increased proportion of CD25$^+$CD44^{low} in *Duxl*-transduced culture was accompanied with a reduced DN2 population. The GFP$^+$CD25$^+$CD44^{low} cells in the *Duxl*-transduced FL cells had a Thy1$^+$ CD11c$^-$ Mac1$^-$NK1.1$^-$B220$^-$ phenotype. We extracted total RNAs from mock-infected DN2 and DN3 and Duxl-introduced DN2 and DN3 cells cultured on OP9-DL1 and analyzed their expression of *Rag1*, *PU.1*, and c-kit using real-time PCR and flow cytometry, respectively. In Duxl-introduced DN2 and DN3 cells, expression of *Rag1* was enhanced and expression of *PU.1* was reduced, whereas no difference was observed in c-kit expression between mock-infected and Duxl-introduced cells (Fig. 5*C*). Therefore, Duxl is supposed to promote the DN2/DN3 transition in some respects, while not in others.

Mock-infected and *Duxl*-transduced CD25$^+$CD44^{low} cells were sorted and their genomic DNA was analyzed by PCR for TCRβ

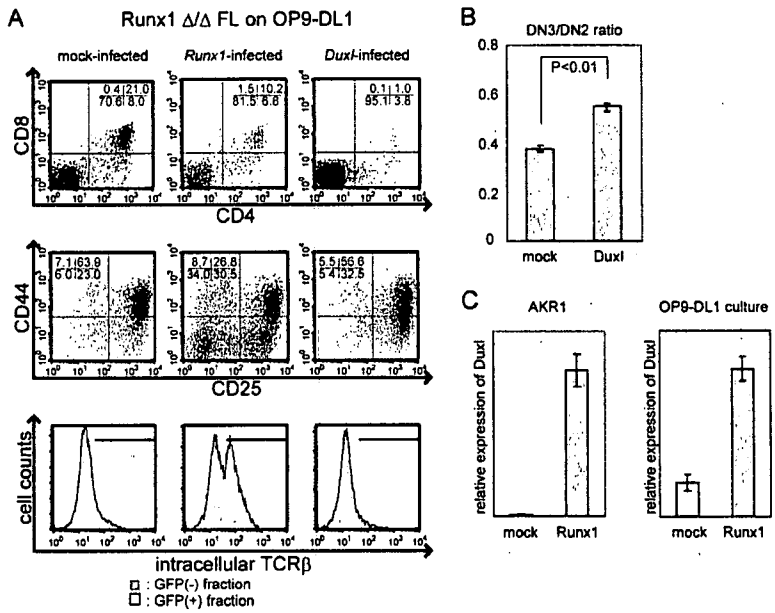

FIGURE 7. Effect of *Duxl* transduction on *Runx1*-deficient FL cells cultured on OP9-DL1. *A*, Expression of CD4/CD8 (*upper panels*), CD25/CD44 (*middle panels*), and iTCRβ (*lower panels*, solid line; GFP^+, gray shade; GFP^-) was examined in OP9-DL1 culture of FL cells harvested from the conditional knockout mice for the *Runx1* gene, in which two floxed alleles of *Runx1* are deleted by Cre recombinase induced from the *Lck* promoter. FL cells were transfected with mock virus (*left*) or with retrovirus expressing *Runx1* (*middle*) or *Duxl* (*right*). Representative FACS analyses are shown. *B*, Average DN3:DN2 ratio of mock-infected and *Duxl*-introduced cells in three independent cultures are shown with ±SD. The two groups were compared using Student's *t* test. *C*, *Runx1* was overexpressed in FL cells or AKR1 cells using retrovirus vector, and the expression levels of *Duxl* in the GFP^+ fraction were examined by qPCR. The amount of transcript of *Duxl* was normalized to the amount of GAPDH RNA in each population and is shown as relative values. Data shown are the average ± SD from triplicate samples.

rearrangement. Interestingly, although the fraction of iTCRβ-positive cells in *Duxl*-transduced DN cells was substantially reduced compared with that in control DN cells (Fig. 5*B*, *lower panels*), the extent of DJβ and V-DJβ rearrangement in *Duxl*-transduced $CD25^+CD44^{low}$ cells was comparable to those of control cells or rather slightly accelerated compared with control cells (Fig. 5*D*), indicating that Duxl actively represses expression of rearranged *TCRβ* genes. Indeed, expression of surface TCRβ in the mouse thymoma cell line AKR1, which exhibits the DP phenotype ($CD4^+CD8^+TCR^{int}$), was reduced after *Duxl* was introduced using retroviral vector (Fig. 5*E*). Taken together, these data suggest that the increased $CD25^+CD44^{low}$ population in the *Duxl*-transduced cells show a DN3a-like phenotype and that constitutive expression of Duxl promotes the DN2/DN3 transition but compromises the process of β selection.

To further investigate the role of Duxl in DN2/DN3 transition, we knocked down the expression of *Duxl* in FL cells using RNA interference, in which FL cells were transfected with a retrovirus that produces shRNA directed against *Duxl* and examined for their development in the OP9-DL1 culture. Among three different shRNAs (sequences 1–3), only sequence 1 shRNA showed significant RNA interference as confirmed by the reduced cell surface expression of a truncated form of nerve growth factor receptor (NGFRt) in NIH3T3, where the NGFRt was translated from a bicistronic message of the *Duxl-IRES-NGFRt* (Fig. 6*A*). When transduced with sequence 1 shRNA, FL cells showed a reduced DN2/DN3 transition in OP9-DL1 culture as determined by the higher levels of CD44 expression in GFP^+CD25^+ cells compared with GFP^- $CD25^+$ cells within the same culture or with GFP^+CD25^+ cells in the *αLuc* (mock)-infected culture (Fig. 6*B*).

It was of particular interest to explore a possible functional link between Duxl and Runx1, because we showed that Runx1 is essential for the DN2/DN3 transition (18). Thus, we tested whether Duxl can rescue the phenotype of Runx1 deficiency in developing thymocytes by transducing *Duxl* into FL cells from *Runx1*-deficient mice in OP9-DL1 culture. Although mock-transduced *Runx1*-deficinet FL cells showed the defective DN2/DN3 transition with impaired down-regulation of CD44 (19), *Duxl* transduction clearly increased the $CD44^{low}CD25^+$ population (Fig. 7, *A* and *B*), although the latter population still did not express intracellular TCRβ chains (Fig. 7*A*, *lower panels*). Thus, *Duxl* can induce down-regulation of CD44 in a *Runx1*-independent manner. We further examined whether *Duxl* is induced by Runx1 or not, where *Runx1* was transduced into normal FL cells in OP9-DL1 culture or an AKR1 cell line, and expression of *Duxl* was measured by quantitative PCR 72 h after the transduction. In both experiments, *Runx1*-transduced GFP^+ cells showed a marked increase in *Duxl* expression (Fig. 7*C*). These results indicated that Runx1 promotes the DN2/DN3 transition by, at least in part, regulating expression of *Duxl*, although it is not clear whether this regulation is direct or indirect.

Discussion

Several groups have investigated the gene expression profiles of developing thymocytes (40–43). Despite the differences in analytical methods, panels of genes to be examined, microarray used, thymocyte subpopulation analyzed, or species, the reported expression pattern of some representative genes such as *pTα*, *Nothc3*, *Egr3*, or *SpiB* were reproduced in our study (15, 40, 42). Furthermore, our study revealed a new aspect that was not described so far and adds to knowledge of the development of thymocytes. Intrathymic development of thymocytes is a dynamic process, during which immature thymocytes progressively commit to mature T cell differentiation accompanied by explosive expansions of their population. As such, we initially expected that this process be driven by induction of a large number of regulatory genes. Unexpectedly, however, our expression profiling clearly showed that gene regulation during early thymocyte development is characterized by mostly repressive activities of transcription, where 90% of the differentially expressed genes were eventually down-regulated. This means that as thymocytes differentiate from their progenitors, they become to use more limited sets of genes at least before differentiating into DP cells.

Among these down-regulated genes, a notable subset is a group of genes that show lineage-promiscuous expression. According to our somewhat arbitrary criteria, these genes account for a substantial proportion (20%) of down-regulated genes in DN2. In other words, immature thymocytes in the DN2 subset simultaneously

express genes from different lineage-affiliated programs. Such lineage-promiscuous states were previously implicated for multipotent hemopoietic progenitors based on the observation for limited numbers of lineage-affiliated genes (44–46). We confirmed this for DN thymocytes by analyzing expression of a large number of genes and also evaluated their temporal changes during the course of their development. Of note is that mature T cell-related genes expressed in DN2 are also transiently repressed during DN2 to DN4 progression. Because our criteria of >10 times higher expression than the median could be too strict, more DN2 genes undergoing down-regulation thereafter could be explained under this framework.

The interpretation of this lineage-promiscuous gene expression in very immature thymocytes is elusive, but it may be speculated that these immature cells are conditioned or primed before their differentiation into particular lineages and that these "primed" states are represented by expression of multiple lineage-affiliated genes. In this scenario, the lineage-promiscuous expression of DN thymocytes could be related to plasticity of these cells. DN2 thymocytes are committed to T lineage to a certain extent but still can give rise to other lineages such as NK cells (10, 12–14), which might reflect the observation that NK cell-affiliated genes were more slowly down-regulated during DN thymocyte development (Fig. 3*C*). Alternatively, lineage-promiscuous gene expression could be explained by the heterogeneous lineage potential at the level of cellular complexity. Because $CD44^{+}LCD25^{low}$ DN1 cells are composed of multiple subsets with distinct differentiation capacity that could be identified with additional c-kit and CD24 staining (11), DN1 cells express a large number of lineage-promiscuous genes down-regulated at the DN1/DN2 transition (40). This may be also the case with DN2 cells we have sorted without c-kit and CD24 staining in this study. Although, the observation that differentiation capacity of DN1 cells with lysozyme expression was similar to that of DN1 cells without lysozyme expression (47) strongly supports the former interpretation, it is necessary to examine the gene expression profiles of each single DN cell, as well as more precise sorting with c-kit and CD24 staining, to know which interpretation is more accurate.

Computational mapping of differentially expressed genes showing similar temporal profiles (CL1–CL6) to known functional pathways seems to be effective to extract the relevant pathways in DN thymocyte development, because it successfully extracted well-characterized pathways in developing thymocytes, such as those related to *Runx1*, *TCRβ*, *NF-κB*, *NFAT*, and *Notch* genes. In addition, it also implicated the presence of several previously unknown pathways that might be regulated during thymocyte development. Although further evaluations are required, finding of these potentially relevant pathways will provide valuable clues to the exploring molecular mechanisms of regulation of DN thymocyte development.

During DN thymocyte development, only a minority of genes was newly induced, among which those included in the CL4 cluster were of our particular interest, because they were transiently expressed within a window in DN3 and contained several well-known pathways and genes that are critical for thymocyte development. From a few candidate genes within this cluster that are potentially involved in transcriptional regulations, we identified a novel double homeobox gene, named *Duxl*, which is transiently expressed in DN3a and could have critical roles in regulation of DN thymocyte development. When constitutively expressed in FL cells in OP9-DL1 culture, Duxl enhances the proportion of $CD44^{low}CD25^{+}$ thymocytes that mimic the phenotype of DN3a cells with severely reduced DP cells, while the knockdown of Duxl in FL cells impaired the proper DN2/DN3 transition. Thus, Duxl is thought to play an important role in promoting the DN2/DN3 transition in the development of DN thymocytes.

In early thymocyte development, Duxl has several functional similarities to SpiB, in that it is highly expressed in DN3a as well as B cells, and that normal thymocyte development is impaired when constitutively expressed or knocked down in early thymocytes (33). These observations may implicate a possible functional link between SpiB and Duxl, which should be addressed in further analysis. For example, SpiB also regulates B cell differentiation, implicating that Duxl is also involved in development of B cells.

Of particular interest is the finding that *Duxl* is induced by Runx1 expression and can partially rescue the *Runx1*-deficient phenotype with regard to the down-regulation of cell surface CD44, indicating that Duxl is one of the effecter molecules involved in the DN2/DN3 transition that is regulated by Runx1. The detailed molecular mechanism of the DN2/DN3 transition is largely unknown because only limited numbers of mice strains, namely, *Runx1*-deficient mice (18) and *pTα/common cytokine receptor γ-chain* double knock-out mice (20), exhibit the maturational block between the DN2 and the DN3 stage. However, considering the fact that during the transition from the DN2 to the DN3 stage, the *TCRβ* gene is rearranged and αβT cell, γδT cell, and NK cell lineages begin to diverge (10, 48, 49), the DN2/DN3 transition, on which our findings could shed light, is supposed to be a crucial developmental step.

On the other hand, the interpretation of the severely reduced production of DP cells associated with constitutive expression of *Duxl* in FL cells is complicated in a context of its physiological roles. Since the *Duxl*-transduced FL cells seem to show a maturational block at the transition between DN3a and DN3b, during which Duxl undergoes down-regulation in vivo, it may be postulated that *Duxl* being normally down-regulated in this step is important for the β selection and subsequent DP thymocyte production. We may safely conclude that the precise regulation of Duxl expression is essential for DP thymocytes to be normally generated in OP9 culture, but its physiological functions in β selection and DP thymocyte generation are still elusive. To address this, more sophisticated experimental approaches with precisely targeted expression of *Duxl* in vivo should be required.

In conclusion, through the gene expression profiling of chronologically discrete subsets of DN thymocytes, we demonstrated the predominantly repressive gene regulation during DN thymocyte development along with its implication in lineage-promiscuous gene expression in immature thymocytes. Among the gene cluster showing transient expression in DN3, we identified *Duxl*, a novel double homeobox gene, that is induced by Runx1 and involved in regulation of DN thymocyte development.

Acknowledgments

We thank J. C. Zúñiga-Pflücker for OP9-DL1 stromal cells, H. Nakauchi for pGCDNsam retroviral vector, M. Miyagishi for designing shRNA, and T. Kitamura for PlatE packaging cells.

Disclosures

The authors have no financial conflict of interest.

References

1. Ceredig, R., and T. Rolink. 2002. A positive look at double-negative thymocytes. *Nat. Rev. Immunol.* 2: 888–897.
2. Pearse, M., L. Wu, M. Egerton, A. Wilson, K. Shortman, and R. Scollay. 1989. A murine early thymocyte developmental sequence is marked by transient expression of the interleukin 2 receptor. *Proc. Natl. Acad. Sci. USA* 86: 1614–1618.
3. Godfrey, D. I., J. Kennedy, T. Suda, and A. Zlotnik. 1993. A developmental pathway involving four phenotypically and functionally distinct subsets of $CD3^{-}CD4^{-}CD8^{-}$ triple-negative adult mouse thymocytes defined by CD44 and CD25 expression. *J. Immunol.* 150: 4244–4252.

4. Penit, C., B. Lucas, and F. Vasseur. 1995. Cell expansion and growth arrest phases during the transition from precursor ($CD4^-8^-$) to immature ($CD4^+8^+$) thymocytes in normal and genetically modified mice. *J. Immunol.* 154: 5103–5113.
5. Godfrey, D. I., J. Kennedy, P. Mombaerts, S. Tonegawa, and A. Zlotnik. 1994. Onset of TCR-β gene rearrangement and role of TCR-β expression during $CD3^-CD4^-CD8^-$ thymocyte differentiation. *J. Immunol.* 152: 4783–4792.
6. Mombaerts, P., A. R. Clarke, M. A. Rudnicki, J. Iacomini, S. Itohara, J. J. Lafaille, L. Wang, Y. Ichikawa, R. Jaenisch, M. L. Hooper, et al. 1992. Mutations in T-cell antigen receptor genes α and β block thymocyte development at different stages. *Nature* 360: 225–231.
7. Shinkai, Y., S. Koyasu, K. Nakayama, K. M. Murphy, D. Y. Loh, E. L. Reinherz, and F. W. Alt. 1993. Restoration of T cell development in RAG-2-deficient mice by functional TCR transgenes. *Science* 259: 822–825.
8. Hoffman, E. S., L. Passoni, T. Crompton, T. M. Leu, D. G. Schatz, A. Koff, M. J. Owen, and A. C. Hayday. 1996. Productive T-cell receptor β-chain gene rearrangement: coincident regulation of cell cycle and clonality during development in vivo. *Genes Dev.* 10: 948–962.
9. Allman, D., A. Sambandam, S. Kim, J. P. Miller, A. Pagan, D. Well, A. Meraz, and A. Bhandoola. 2003. Thymopoiesis independent of common lymphoid progenitors. *Nat. Immunol.* 4: 168–174.
10. Schmitt, T. M., M. Ciofani, H. T. Petrie, and J. C. Zúñiga-Pflücker. 2004. Maintenance of T cell specification and differentiation requires recurrent notch receptor-ligand interactions. *J. Exp. Med.* 200: 469–479.
11. Porritt, H. E., L. L. Rumfelt, S. Tabrizifard, T. M. Schmitt, J. C. Zúñiga-Pflücker, and H. T. Petrie. 2004. Heterogeneity among DN1 prothymocytes reveals multiple progenitors with different capacities to generate T cell and non-T cell lineages. *Immunity* 20: 735–745.
12. Ikawa, T., H. Kawamoto, S. Fujimoto, and Y. Katsura. 1999. Commitment of common T/natural killer (NK) progenitors to unipotent T and NK progenitors in the murine fetal thymus revealed by a single progenitor assay. *J. Exp. Med.* 190: 1617–1626.
13. Wu, L., C. L. Li, and K. Shortman. 1996. Thymic dendritic cell precursors: relationship to the T lymphocyte lineage and phenotype of the dendritic cell progeny. *J. Exp. Med.* 184: 903–911.
14. Manz, M. G., D. Traver, T. Miyamoto, I. L. Weissman, and K. Akashi. 2001. Dendritic cell potentials of early lymphoid and myeloid progenitors. *Blood* 97: 3333–3341.
15. David-Fung, E. S., M. A. Yui, M. Morales, H. Wang, T. Taghon, R. A. Diamond, and E. V. Rothenberg. 2006. Progression of regulatory gene expression states in fetal and adult pro-T-cell development. *Immunol. Rev.* 209: 212–236.
16. Radtke, F., A. Wilson, G. Stark, M. Bauer, J. van Meerwijk, H. R. MacDonald, and M. Aguet. 1999. Deficient T cell fate specification in mice with an induced inactivation of Notch1. *Immunity* 10: 547–558.
17. Michie, A. M., and J. C. Zúñiga-Pflücker. 2002. Regulation of thymocyte differentiation: pre-TCR signals and β-selection. *Semin. Immunol.* 14: 311–323.
18. Ichikawa, M., T. Asai, T. Saito, G. Yamamoto, S. Seo, I. Yamazaki, T. Yamagata, K. Mitani, S. Chiba, H. Hirai, et al. 2004. AML-1 is required for megakaryocytic maturation and lymphocytic differentiation, but not for maintenance of hematopoietic stem cells in adult hematopoiesis. *Nat. Med.* 10: 299–304.
19. Kawazu, M., T. Asai, M. Ichikawa, G. Yamamoto, T. Saito, S. Goyama, K. Mitani, K. Miyazono, S. Chiba, S. Ogawa, et al. 2005. Functional domains of Runx1 are differentially required for CD4 repression, TCRβ expression, and CD4/8 double-negative to CD4/8 double-positive transition in thymocyte development. *J. Immunol.* 174: 3526–3533.
20. Di Santo, J. P., I. Aifantis, E. Rosmaraki, C. Garcia, J. Feinberg, H. J. Fehling, A. Fischer, H. von Boehmer, and B. Rocha. 1999. The common cytokine receptor γ chain and the pre-T cell receptor provide independent but critically overlapping signals in early $\alpha\beta$ T cell development. *J. Exp. Med.* 189: 563–574.
21. Li, C., and W. H. Wong. 2001. Model-based analysis of oligonucleotide arrays: expression index computation and outlier detection. *Proc. Natl. Acad. Sci. USA* 98: 31–36.
22. Li, C., and W. H. Wong. 2001. Model-based analysis of oligonucleotide arrays: model validation, design issues and standard error application. *Genome Biol.* 2: 0032.0031–0032.0011.
23. Tusher, V. G., R. Tibshirani, and G. Chu. 2001. Significance analysis of microarrays applied to the ionizing radiation response. *Proc. Natl. Acad. Sci. USA* 98: 5116–5121.
24. de Hoon, M. J., S. Imoto, J. Nolan, and S. Miyano. 2004. Open source clustering software. *Bioinformatics* 20: 1453–1454.
25. Herrero, J., F. Al-Shahrour, R. Diaz-Uriarte, A. Mateos, J. M. Vaquerizas, J. Santoyo, and J. Dopazo. 2003. GEPAS: A web-based resource for microarray gene expression data analysis. *Nucleic Acids Res.* 31: 3461–3467.
26. Herrero, J., J. M. Vaquerizas, F. Al-Shahrour, L. Conde, A. Mateos, J. S. Diaz-Uriarte, and J. Dopazo. 2004. New challenges in gene expression data analysis and the extended GEPAS. *Nucleic Acids Res.* 32: W485–W491.
27. Sato, H., S. Ishida, K. Toda, R. Matsuda, Y. Hayashi, M. Shigetaka, M. Fukuda, Y. Wakamatsu, and A. Itai. 2005. New approaches to mechanism analysis for drug discovery using DNA microarray data combined with KeyMolnet. *Curr. Drug Discov. Technol.* 2: 89–98.
28. Boyle, E. I., S. Weng, J. Gollub, H. Jin, D. Botstein, J. M. Cherry, and G. Sherlock. 2004. GO: Termfinder–open source software for accessing gene ontology information and finding significantly enriched gene ontology terms associated with a list of genes. *Bioinformatics* 20: 3710–3715.
29. Schmitt, T. M., and J. C. Zúñiga-Pflücker. 2002. Induction of T cell development from hematopoietic progenitor cells by delta-like-1 in vitro. *Immunity* 17: 749–756.
30. Anderson, S. J., K. M. Abraham, T. Nakayama, A. Singer, and R. M. Perlmutter. 1992. Inhibition of T-cell receptor β-chain gene rearrangement by overexpression of the non-receptor protein tyrosine kinase $p56^{lck}$. *EMBO J.* 11: 4877–4886.
31. Miyagishi, M., and K. Taira. 2003. Strategies for generation of an siRNA expression library directed against the human genome. *Oligonucleotides* 13: 325–333.
32. Su, A. I., T. Wiltshire, S. Batalov, H. Lapp, K. A. Ching, D. Block, J. Zhang, R. Soden, M. Hayakawa, G. Kreiman, M. P. Cooke, et al. 2004. A gene atlas of the mouse and human protein-encoding transcriptomes. *Proc. Natl. Acad. Sci. USA* 101: 6062–6067.
33. Lefebvre, J. M., M. C. Haks, M. O. Carleton, M. Rhodes, G. Sinnathamby, M. C. Simon, L. C. Eisenlohr, L. A. Garrett-Sinha, and D. L. Wiest. 2005. Enforced expression of Spi-B reverses T lineage commitment and blocks β-selection. *J. Immunol.* 174: 6184–6194.
34. Carleton, M., M. C. Haks, S. A. Smeele, A. Jones, S. M. Belkowski, M. A. Berger, P. Linsley, A. M. Kruisbeek, and D. L. Wiest. 2002. Early growth response transcription factors are required for development of $CD4^-CD8^-$ thymocytes to the $CD4^+CD8^+$ stage. *J. Immunol.* 168: 1649–1658.
35. Miyazaki, T. 1997. Two distinct steps during thymocyte maturation from $CD4^-CD8^-$ to $CD4^+CD8^+$ distinguished in the early growth response (Egr)-1 transgenic mice with a recombinase-activating gene-deficient background. *J. Exp. Med.* 186: 877–885.
36. Xi, H., R. Schwartz, I. Engel, C. Murre, and G. J. Kersh. 2006. Interplay between RORγt, Egr3, and E proteins controls proliferation in response to pre-TCR signals. *Immunity* 24: 813–826.
37. Bellavia, D., A. F. Campese, A. Vacca, A. Gulino, and I. Screpanti. 2003. Notch3, another Notch in T cell development. *Semin. Immunol.* 15: 107–112.
38. Booth, H. A., and P. W. Holland. 2007. Annotation, nomenclature, and evolution of four novel homeobox genes expressed in the human germ line. *Gene* 387: 7–14.
39. Taghon, T., M. A. Yui, R. Pant, R. A. Diamond, and E. V. Rothenberg. 2006. Developmental and molecular characterization of emerging β- and $\gamma\delta$-selected pre-T cells in the adult mouse thymus. *Immunity* 24: 53–64.
40. Tabrizifard, S., A. Olaru, J. Plotkin, M. Fallahi-Sichani, F. Livak, and H. T. Petrie. 2004. Analysis of transcription factor expression during discrete stages of postnatal thymocyte differentiation. *J. Immunol.* 173: 1094–1102.
41. Huang, Y. H., D. Li, A. Winoto, and E. A. Robey. 2004. Distinct transcriptional programs in thymocytes responding to T cell receptor, Notch, and positive selection signals. *Proc. Natl. Acad. Sci. USA* 101: 4936–4941.
42. Dik, W. A., K. Pike-Overzet, F. Weerkamp, D. de Ridder, E. F. de Haas, M. R. Baert, P. van der Spek, E. E. Koster, M. J. Reinders, J. J. van Dongen, et al. 2005. New insights on human T cell development by quantitative T cell receptor gene rearrangement studies and gene expression profiling. *J. Exp. Med.* 201: 1715–1723.
43. Hoffmann, R., L. Bruno, T. Seidl, A. Rolink, and F. Melchers. 2003. Rules for gene usage inferred from a comparison of large-scale gene expression profiles of T and B lymphocyte development. *J. Immunol.* 170: 1339–1353.
44. Akashi, K., D. Traver, T. Miyamoto, and I. L. Weissman. 2000. A clonogenic common myeloid progenitor that gives rise to all myeloid lineages. *Nature* 404: 193–197.
45. Hu, M., D. Krause, M. Greaves, S. Sharkis, M. Dexter, C. Heyworth, and T. Enver. 1997. Multilineage gene expression precedes commitment in the hemopoietic system. *Genes Dev.* 11: 774–785.
46. Nutt, S. L., B. Heavey, A. G. Rolink, and M. Busslinger. 1999. Commitment to the B-lymphoid lineage depends on the transcription factor Pax5. *Nature* 401: 556–562.
47. Laiosa, C. V., M. Stadtfeld, H. Xie, L. de Andres-Aguayo, and T. Graf. 2006. Reprogramming of committed T cell progenitors to macrophages and dendritic cells by C/EBPα and PU.1 transcription factors. *Immunity* 25: 731–744.
48. Ciofani, M., G. C. Knowles, D. L. Wiest, H. von Boehmer, and J. C. Zúñiga-Pflücker. 2006. Stage specific and differential notch dependency at the $\alpha\beta$ and $\gamma\delta$ T lineage bifurcation. *Immunity* 25: 105–116.
49. Prinz, I., A. Sansoni, A. Kissenpfennig, L. Ardouin, M. Malissen, and B. Malissen. 2006. Visualization of the earliest steps of $\gamma\delta$ T cell development in the adult thymus. *Nat. Immunol.* 7: 995–1003.

Journal of Medical Virology 79:811–819 (2007)

Prophylactic Effects of Chitin Microparticles on Highly Pathogenic H5N1 Influenza Virus

Takeshi Ichinohe,[1,2†] Noriyo Nagata,[1] Peter Strong,[3] Shin-ichi Tamura,[1] Hidehiro Takahashi,[1] Ai Ninomiya,[4] Masaki Imai,[4] Takato Odagiri,[4] Masato Tashiro,[4] Hirofumi Sawa,[5] Joe Chiba,[2] Takeshi Kurata,[1] Tetsutaro Sata,[1] and Hideki Hasegawa[1*]

[1]*Department of Pathology, National Institute of Infectious Diseases, Gakuen, Musashimurayama-shi, Tokyo, Japan*
[2]*Department of Biological Science and Technology, Tokyo University of Science, Yamazaki, Noda, Chiba, Japan*
[3]*CMP Therapeutics Ltd., Oxford, UK*
[4]*Department of Virology III, National Institute of Infectious Diseases, Gakuen, Musashimurayama-shi, Tokyo, Japan*
[5]*Department of Molecular Pathobiology, 21st Century COE Program for Zoonosis Control, Hokkaido University Research Center for Zoonosis Control, Kita-ku, Sapporo, Japan*

Highly pathogenic avian influenza virus (H5N1) is an emerging pathogen with the potential to cause great harm to humans, and there is concern about the potential for a new influenza pandemic. This virus is resistant to the antiviral effects of interferons and tumor necrosis factor-α. However, the mechanism of interferon-independent protective innate immunity is not well understood. The prophylactic effects of chitin microparticles as a stimulator of innate mucosal immunity against a recently obtained strain of H5N1 influenza virus infection were examined in mice. Clinical parameters and the survival rate of mice treated by intranasal application of chitin microparticles were significantly improved compared to non-treated mice after a lethal influenza virus challenge. Flow cytometric analysis revealed that the number of natural killer cells that expressed tumor necrosis factor-related apoptosis-inducing ligand (TRAIL) and that had migrated into the cervical lymph node was markedly increased (26-fold) after intranasal treatment with chitin microparticles. In addition, the level of IL-6 and interferon-gamma-inducible protein-10 (IP-10) in the nasal mucosa after H5N1 influenza virus challenge was decreased by prophylactic treatment with chitin microparticles. These results suggest that prophylactic intranasal administration of chitin microparticles enhanced the local accumulation of natural killer cells and suppressed hyper-induction of cytokines, resulting in an innate immune response to prevent pathogenesis of H5N1 influenza virus. ***J. Med. Virol. 79:811–819, 2007.***

KEY WORDS: influenza virus H5N1; innate immunity; chitin

INTRODUCTION

Avian influenza A subtype H5N1 outbreaks involving fatal human respiratory disease were reported in Hong Kong in 1997 (H5N1/97) [Claas et al., 1998; Subbarao et al., 1998]. The subsequent re-emergence of human H5N1 disease with high fatality rates has been reported in southern China [Peiris et al., 2004], Vietnam [Tran et al., 2004], Thailand [Grose and Chokephaibulkit, 2004], Cambodia, Indonesia, Turkey, and Iraq. At least 278 laboratory-confirmed cases of human infection with a fatality rate of greater than 50% were reported to the World Health Organization [2007] from January 2003 to March 2007. It has been reported that an oseltamivir-resistant H5N1 influenza virus (A/Hanoi/30408/2005) was isolated from a Vietnamese girl [Le et al., 2005], and H5N1 influenza viruses isolated from Hong Kong (A/Hong Kong/156/97, A/Hong Kong/483/97, and A/Hong Kong/486/97) were resistant to the antiviral effects of interferons and tumor necrosis factor-α [Seo et al., 2002].

Natural killer cells eliminate tumor cells and cells infected by viruses, including influenza virus, via their cytotoxic activity and production of cytokines [Biron and Brossay, 2001; Cooper et al., 2001; Gazit et al., 2006]. Natural killer cells are rapidly recruited to sites of infection, and can inhibit viral replication and dissemination through the respiratory tract

†Research Fellow of the Japanese Society for the Promotion of Science.

*Correspondence to: Hideki Hasegawa, Department of Pathology, National Institute of Infectious Diseases 4-7-1 Gakuen, Musashimurayama-shi, Tokyo 208-0011, Japan.
E-mail: hasegawa@nih.go.jp

Accepted 5 February 2007
DOI 10.1002/jmv.20837
Published online in Wiley InterScience (www.interscience.wiley.com)

[Stein-Streilein et al., 1983; Stein-Streilein and Guffee, 1986, and unpublished data by P. Strong]. Thus, natural killer cells play a role in the early stage of host defense against viral infection, and also bridge the subsequent adaptive anti-viral immune responses [Kos and Engleman, 1996; Biron, 1997; Biron et al., 1999; Andoniou et al., 2005; O'Leary et al., 2006]. Although the precise mechanism of the innate immune response to highly pathogenic H5N1 influenza virus is still unknown, the role of natural killer cells in innate immunity against viral infection seems to be important.

Chitin (a natural polysaccharide of *N*-acetyl-D-glucosamine), one of the most abundant polysaccharides in nature, is an essential component of fungal walls and the exoskeletons of crabs, shrimp, and insects. Chitin is non-allergenic, non-toxic, bio-degradable and biocompatible. Chitin-derived products are now widely used in the medical, veterinary, cosmetic, health supplement, and environmental industries [Okamoto et al., 1993]. Chitosan, a highly deacetylated form of chitin, has been used as a vaccine adjuvant due to its muco-adhesive properties, and has been shown to enhance antibody responses to mucosally delivered vaccine antigens [Bacon et al., 2000]. Chitin microparticles (1–20 μm in diameter), in contrast to chitosan, have strong immunomodulatory properties. Previous studies showed that chitin microparticles had effective adjuvant activity with an inactivated influenza vaccine [Hasegawa et al., 2005] or with an HIV-DNA vaccine [Hamajima et al., 2003]. Chitin microparticles, when administered intranasally, have also been found to reduce symptoms of respiratory allergy and allergic asthma [Strong et al., 2002; Ozdemir et al., 2006]. Other studies using chitin microparticles have demonstrated their Th1-inducing properties and shown that phagocytosis of chitin microparticles by macrophages through involves the mannose receptor and results in the production of IL-12, IL-18, and tumor necrosis factor-α, which in turn stimulated natural killer cells to produce IFN-γ [Shibata et al., 1997a,b, 1998].

In the present study, prophylactic use of intranasally applied chitin microparticles to stimulate innate mucosal immunity to lethal H5N1 influenza virus challenge is investigated. It is shown that intranasal pretreatment with chitin microparticles induces expression of tumor necrosis factor-related apoptosis-inducing ligand (TRAIL) in a large proportion of natural killer cells in the cervical lymph node, and suppresses viral load and hyper-induction of cytokines that may play a role in the pathogenesis of H5N1 [Chan et al., 2005; de Jong et al., 2006].

MATERIALS AND METHODS

Mice

Six- to 8-week-old female BALB/c mice were purchased from Japan SLC. Mice were kept under specific-pathogen-free conditions approved by the Institution Animal Care and Use Committee of National Institute of Infectious Diseases.

Viruses

The mouse-adapted strains of A/Puerto Rico/8/34 (A/PR8, H1N1) and wild-type A/Vietnam/1194/04 (VN1194, H5N1) viruses were used in this study. The A/PR8 virus was passaged 148 times in the ferret, 596 times in the mouse, and 73 times in 10-day fertile chicken eggs. The VN1194 virus isolated from patients with H5N1 disease in Vietnam in 2004 was prepared in Mardin-Darby canine kidney (MDCK) cells without any additional special steps for mouse adaptation. These viruses were stored at −80°C and viral titers were quantified by plaque assay.

Preparation of Chitin Microparticles, Poly(I:C) and LPS

Chitin microparticles prepared from shrimp derived chitin was kindly provided by P. Strong (CMP Therapeutics Ltd., Oxford, UK). Particle size was determined by Christison Particle Technologies (Gateshead, UK) using a Model 780 Accusizer and the average particle size was 10 μm. The sterility of the chitin microparticles was confirmed by plating on agar plates. The concentration of endotoxin in the chitin microparticles preparations was examined by Limulus Amebocyte Lysate Assay (BioWhittaker, Wokingham, UK) and shown to be less than 1 EU/ml. Synthetic dsRNA [poly(I:C)] was kindly provided by Toray Industries, Inc. (Kamakura, Kanagawa, Japan). Lipopolysaccharide (LPS) was purchased from Sigma (St. Louis, MO).

Pretreatment with Chitin Microparticles, Poly(I:C) and LPS and Virus Infection in Mice

To assess the efficacy of intranasal pretreatment with innate immune stimulators as prophylactic agents against influenza (A/PR8, H1N1) and highly pathogenic avian influenza (VN1194, H5N1) strains, chitin microparticles (100 μg), poly(I:C) (10 μg), LPS (1 μg) or PBS were administered intranasally to mice. CMP treatments were performed once a day for 2 or 3 days and other treatments were performed once (6 hr) before viral challenge. Previous experiments established the optimum dosing schedule for CMP, poly(I:C), and LPS. These amounts of each of the innate stimulators were sufficient to generate adjuvant activity against influenza virus infection when they were administered intranasally with vaccine [Ichinohe et al., 2005, 2006]. Five mice for each experimental group were anesthetized with diethyl ether and received an intranasal application of 10 μl of PBS containing chitin microparticles, poly(I:C) or LPS (5 μl/each nostril) prior to influenza virus infection. Mice were anesthetized 6 hr after final administration, and 2 μl of a suspension of influenza virus (A/PR8 or VN1194) was dropped into each nostril (4 μl per mouse). Virus titers of nasal washes were measured 3 days after inoculation of the influenza virus. H5N1 virus infection experiments were carried out in biosafety level 3 containment facilities approved

by the Guides for Animal Experiments Performed at the National Institute of Infectious Diseases.

Titration of Virus

Mice were given 100 μg of chitin microparticles or PBS twice intranasally at 30 and 6 hr before infection, then infected with 1,000 PFU of H5N1 influenza virus. Mice (n = 3 mice per time point) were sacrificed and tissues were collected 3, 5, 8, or 10 days post-infection. Viral titration in the frontal lobe, trigeminal nerve ganglia, brain stem, cervical lymph node, spleen, liver, kidney, large intestine, muscle, serum, nasal wash, and lung wash of infected mice was determined by plaque assay using MDCK cells (Fig. 4). Lung washes and nasal washes were prepared in PBS containing 0.1% bovine serum albumin, as described previously [Asahi et al., 2002] and used for viral titration after removing cellular debris by centrifugation. Tissue homogenates (1–10%, w/v) were prepared in PBS containing 0.1% bovine serum albumin, centrifuged at 9,170*g* for 10 min, and supernatants were inoculated into cells in the presence of 10 μg/ml acetylated trypsin (Sigma).

Flow Cytometry

Mice were given 100 μg of chitin microparticles intranasally once a day for 3 days, and sacrificed 6 hr after the final administration to collect the cervical lymph node. The number of natural killer cells in the local lymphoid tissue was analyzed by three-color flow cytometry. Single cell suspensions were prepared from the cervical lymph node and red blood cells were depleted by incubation in 0.83% NH_4Cl. Cells were incubated with 5 μg/ml of anti-mouse CD16/32 antibody (eBioscience, San Diego, CA) to block nonspecific binding, then incubated with FITC-labeled anti-mouse pan-natural killer cell antibody (Dx5, eBioscience) and phycoerythrin (PE)-labeled anti-mouse tumor necrosis factor-related apoptosis-inducing ligand (TRAIL) antibody (N2B2, eBioscience). To quantitate the total number of live cells an aliquot of cells were incubated with propidium iodide (PI, final concentration; 5 μg/ml). Samples were analyzed with a flow cytometer (FACS-Calibur, BD Biosciences, San Jose, CA), and the data were analyzed with CELLQuest software.

Multiplex Cytokine Assays

Mice were given 100 μg of chitin microparticles or PBS intranasally once a day for 2 days, then infected with 1,000 PFU of H5N1 influenza virus. After the challenge, mice were sacrificed to collect nasal washes at 3, 5, 8, or 10 days post-infection. Samples of nasal washes were analyzed for 20 cytokines (FGF basic, GM-CSF, IFN-γ, IL-1α, IL-1β, IL-2, IL-4, IL-5, IL-6, IL-10, IL-12, IL-13, IL-17, IP-10, KC, MCP-1, MIG, MIP-1α, TNF-α, and VEGF) by Luminex 200™ (Luminex Co., Austin, TX) using mouse cytokine twenty-plex antibody bead kit (BioSource International, Inc. Camarillo, CA), according to the manufacturer's instructions. Briefly, Multiplex beads were vortexed and sonicated for 30 s and 25 μl of beads suspension was added to each well of a 96 well filter plate and washed twice with wash buffer. The nasal wash were diluted 1:1 in assay diluent and loaded onto a Millipore Multiscreen BV 96-well filter plate to which 50 μl of incubation buffer had been added to each well. Serial dilutions of cytokines standards were prepared in parallel and added to the plate. Samples were incubated on a plate shaker in the dark at room temperature for 2 hr. The plate was applied to a Millipore Multiscreen Vacuum Manifold, washed twice with 200 μl wash buffer, and 100 μl of biotinylated Anti-Mouse Multi-Cytokine Detector Antibody was added to each well. The plate was shaken again as above for 1 hr applied to a Millipore Multiscreen Vacuum Manifold, and washed twice with 200 μl wash buffer. One hundred microliters of Streptavidin R-phycoerythrin was added directly to each well, plate was shaken again as above for 30 min, applied to the vacuum manifold, and washed twice. One hundred microliters of wash buffer was added to each well and the plate was shaken for 3 min. The assay plate was analyzed using the Bio-Plex Luminex 100 XYP instrument. Cytokine concentrations were calculated using Bio-Plex Manager 3.0 software with a five parameter curve-fitting algorithm applied for standard curve calculation.

Statistics

Comparisons between experimental groups were made using the Student's *t*-test for paired observations; $P < 0.05$ was considered statistically significant.

RESULTS

Protective Effect of Chitin Microparticles on A/PR8 (H1N1) or A/Vietnam (H5N1) Influenza virus Infection

To assess the efficacy of intranasal pretreatment with chitin microparticles as a prophylactic treatment against avirulent (A/PuertoRico/8/34/, H1N1) or highly pathogenic avian influenza virus infection (A/Vietnam/1194/2004, H5N1), a chitin microparticle suspension was given intranasally to mice. After H1N1 viral challenge, mice pretreated intranasally with either poly(I:C) or LPS given 6 hr prior to infection showed a marked reduction in virus titer in their nasal wash (Fig. 1A). Mice treated with three daily doses of CMP showed a partial but significant reduction of nasal-wash virus titers (Fig. 1A). The protective effect of chitin microparticles against H5N1 influenza virus infection was also examined. Mice treated intranasally with three daily doses of chitin microparticles showed a marked reduction in virus titer in their nasal washes, although mice pretreated with either poly(I:C) or LPS showed only a partial reduction in virus titers in their nasal

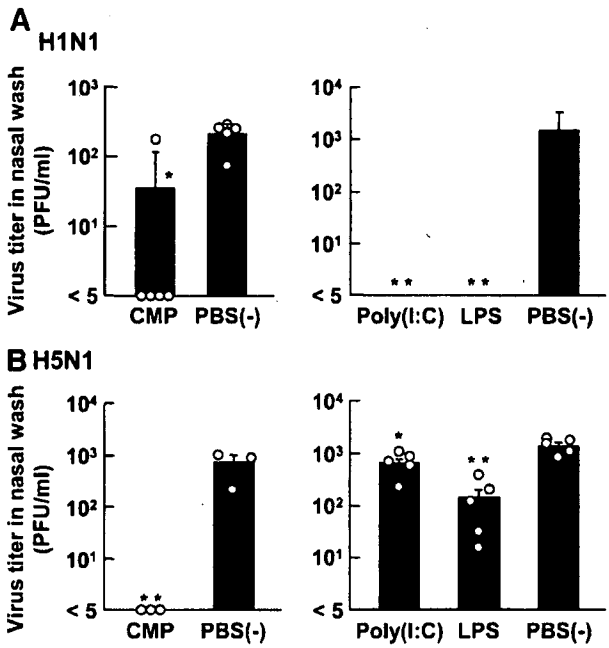

Fig. 1. Protective effect of innate immune stimulators against H1N1 and H5N1 influenza virus infection in BALB/c mice. **A**: Mice (n = 5 mice per group) received 100 μg of chitin microparticles (CMP) once a day for 3 days, or 10 μg of poly(I:C), 1 μg of LPS, or PBS once 6 hr before viral challenge, then were infected intranasally with 100 PFU of A/PR8 (H1N1) influenza viruses in 2 μl suspension for each nostril. Virus titers in nasal washes 3 days post-inoculation are shown. **B**: Mice were pretreated as above and infected intranasally with 1,000 PFU of VN1194 (H5N1) influenza viruses in 2 μl suspension for each nostril. Virus titers in nasal washes 3 days post-inoculation are shown. Data represents the means ± standard error (SE). Open circles indicate values for individual mice. Asterisks indicate significant differences compared with infected controls: $^{*}P < 0.05$; $^{**}P < 0.01$.

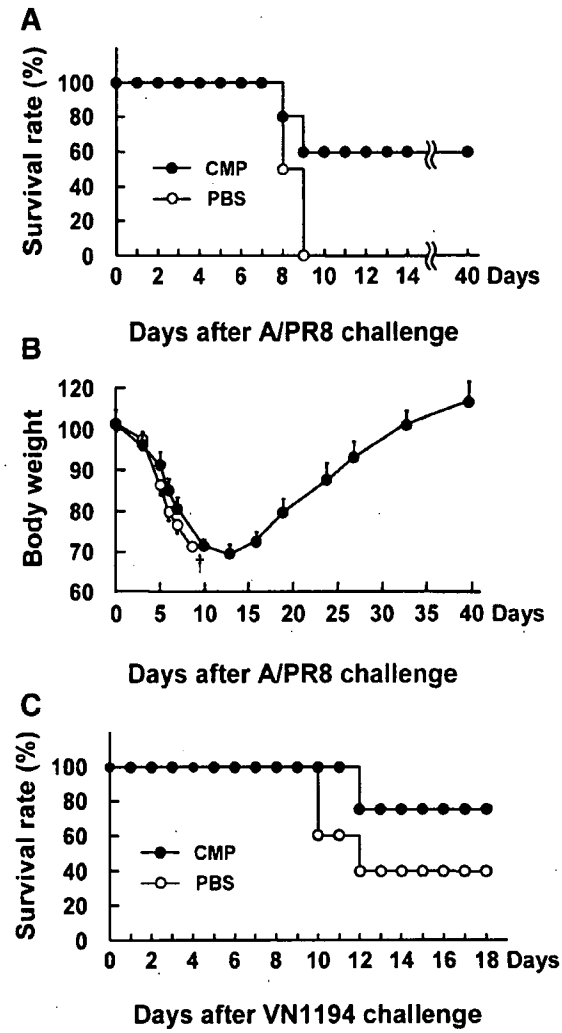

Fig. 2. Prophylactic effect of chitin microparticles (CMP) against H1N1-induced pneumonia or H5N1 influenza virus infection. Mice (n = 4–5 mice per group) were administered 100 μg of chitin microparticles to the lung intranasally in a volume of 20 μl PBS once a day for 3 days (closed circles) or PBS (open circles), then challenged with a lethal dose (4 LD50) of A/PR8/H1N1 influenza virus in 20 μl PBS to the lung. Survival curves (**A**) and body weight changes over time (**B**) after virus challenge are shown. Body weights are plotted as a percentage of the average initial weight. The open cross indicates the time-point at which all mice in a group succumbed to disease. Infected mice were monitored for 40 days. **C**: Mice (n = 5 mice per group) received 100 μg of chitin microparticles once a day for 2 days (closed circles), or PBS (open circles), then infected intranasally with 1,000 PFU of VN1194 (H5N1) influenza virus in 2 μl suspension for each nostril. Survival curves after virus challenge are shown. The survival rates were monitored for 18 days.

washes (Fig. 1B). These results suggest that chitin microparticles can stimulate an immunological reaction that leads to reduction of viral replication in vivo.

Pretreatment With Chitin Microparticles Protects Mice From Lethal Infection of H1N1 and H5N1

The mortality of mice after inoculation with a lethal dose of H1N1 or H5N1 influenza virus was monitored. Chitin microparticles (100 μg) was given intranasally once a day for 3 days before infection with 100 PFU (4 LD50) of H1N1 virus in a 20 μl suspension (Fig. 2A,B). All the control mice pre-treated with PBS were dead 9 days after infection, with marked clinical symptoms of disease and marked reduction of body weight. Mice pretreated with chitin microparticles also lost weight and developed clinical symptoms, but 15 days after infection, 60% of mice recovered their body weight, and survived for the duration of the experiment (at least 40 days after infection).

The prophylactic effect of chitin microparticles against lethal H5N1 influenza virus infection was also examined. Mice were given 100 μg of chitin microparticles intranasally once a day for 2 days, or PBS 6 hr before intranasal infection with 1,000 PFU of H5N1 influenza viruses. Interestingly, intranasal administration of chitin microparticles led to a significant improvement in survival and fewer clinical symptoms compared with PBS-treated control mice (Fig. 2C). These results suggested that intranasal pretreatment with chitin microparticles protects mice against both H1N1 and H5N1 lethal infections.

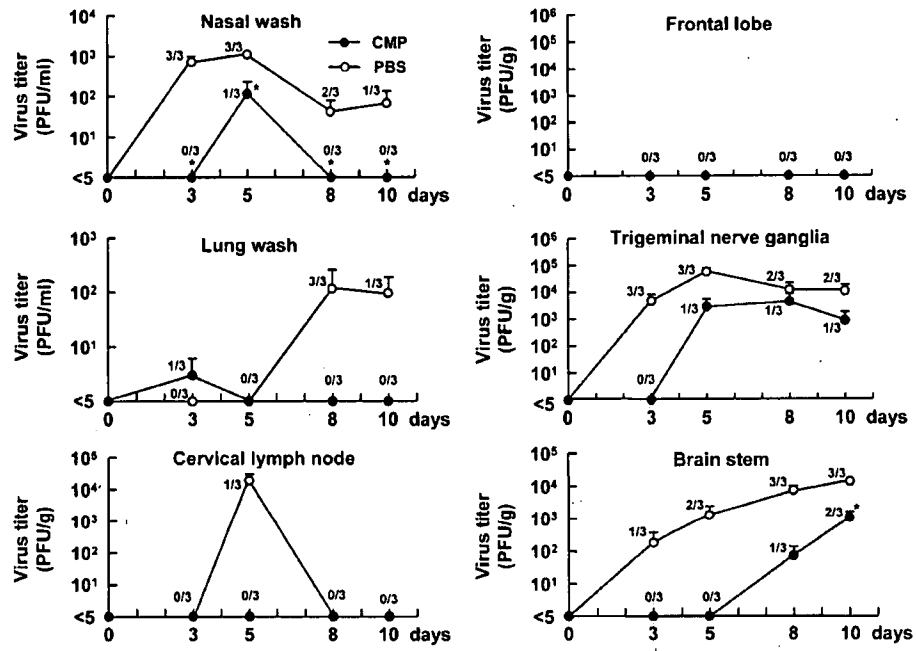

Fig. 3. Virus titers in various organs after challenge with 1,000 PFU of VN1194 (H5N1). Mice were administered 100 μg of chitin microparticles (CMP) intranasally once a day for 2 days (closed circle) or PBS (open circle), and infected with 1,000 PFU of VN1194 influenza virus. Mice were sacrificed to collect organs 3, 5, 8, or 10 days post-inoculation. Virus titers in the indicated organs after viral challenge are shown. Data represents the means ± SE, and represents the numbers of mice that failed to clear viruses/total number of mice (n = 3). Asterisks indicate significant differences compared to the PBS control group; $P < 0.05$.

Reduction of H5N1 Influenza Virus Titer in Multiple Organs by Pretreatment with Chitin Microparticles

To examine the efficiency of viral spread of A/Vietnam/1194/04 (H5N1) after nasal infection in mice, viral titers in multiple tissues from mice intranasally infected with 1,000 PFU of H5N1 were measured 3, 5, 8, and 10 days after infection with or without chitin microparticles pretreatment (n = 3 mice per time point). Mice were given 100 μg of chitin microparticles or PBS intranasally twice at 30 and 6 hr before infection, then infected with 1,000 PFU of H5N1 influenza viruses. When the mice were infected with a small volume (2 μl in each nostil) of virus suspension without chitin microparticles pretreatment, virus titers were detected in nasal washes and in the trigerminal nerve ganglia of all mice 3 days post-inoculation, and were highest at 5 days post-inoculation (open circles in Fig. 3). Thereafter, virus was detected in the lung and brain stem 8 days post-inoculation (open circles in Fig. 3). Interestingly, live virus was not detected in the frontal lobe of the cerebrum, which is directly connected to the nasal cavity via the olfactory nerve. No live virus was detected in the spleen, liver, kidney, large intestine, muscle, or serum of mice (data not shown).

In the nasal wash and brain stem of chitin microparticles-treated mice, the virus titer was significantly reduced compared to PBS-treated mice (closed circles in Fig. 3). In addition, virus titers tended to be much lower in lung washes, cervical lymph node, and terminal nerve ganglia in the chitin microparticles-treated group compared to the control group (closed circles in Fig. 3). Live virus titers were not detected in the frontal lobe of the cerebrum.

Migration of Natural Killer Cells Expressing Tumor Necrosis Factor-Related Apoptosis-Inducing Ligand (TRAIL) in the Cervical Lymph Node After Intranasal Administration of Chitin Microparticles

Previous work suggested that chitin microparticles given intranasally induced an accumulation of natural killer cells in local lymphoid tissue (unpublished data). To define the mechanism of the protective effect of chitin microparticles against highly pathogenic H5N1 influenza virus infection, the migration of natural killer cells into the cervical lymph node was examined. The proportion of natural killer cells in the cervical lymph node increased 6-fold in chitin microparticles-treated mice compared with PBS-treated mice 6 hr after chitin microparticles administration (Fig. 4A). As tumor necrosis factor-related apoptosis-inducing ligand (TRAIL) plays an important role in the immune response of natural killer cells to influenza virus infection [Ishikawa et al., 2005], the number of natural killer cells expressing tumor necrosis factor-related apoptosis-inducing ligand (TRAIL) on their cell surface was counted. The number of tumor necrosis factor-

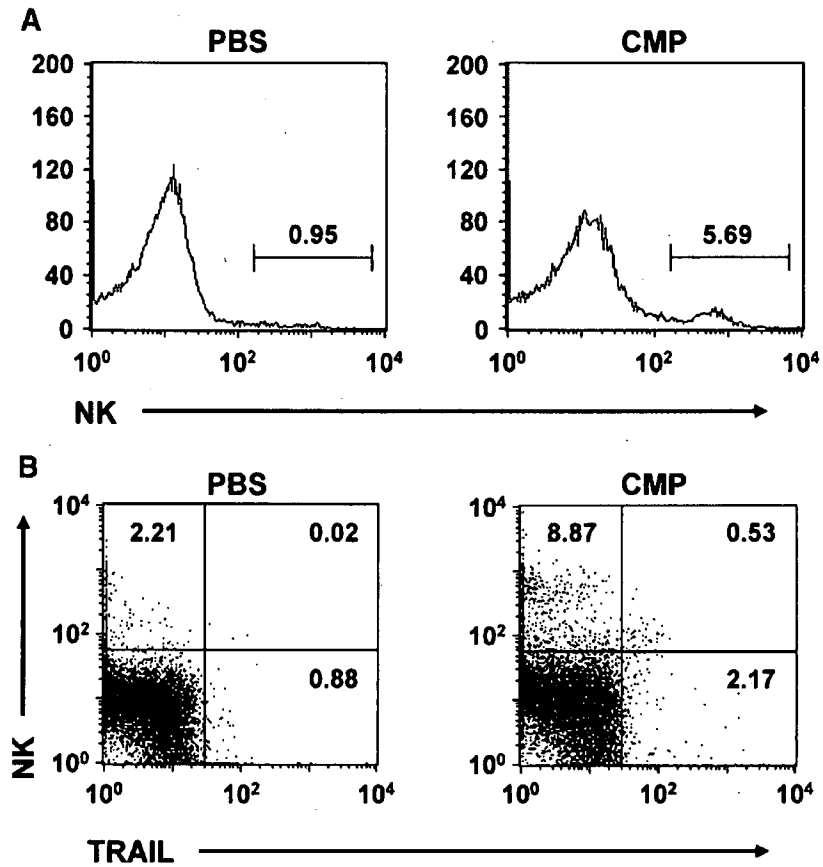

Fig. 4. Increased natural killer (NK) cell migration into the cervical lymph node after intranasal chitin microparticles (CMP) treatment. Mice were administered 100 μg of chitin microparticles intranasally once a day for 3 days or PBS, and sacrificed to collect the cervical lymph node 6 hr after the final administration. cervical lymph node cells of 5 mice were pooled and stained with PI and anti-mouse CD49bFITC and/or anti-mouse tumor necrosis factor-related apoptosis-inducing ligand (TRAIL) PE antibodies. Viable cells (PI−) were selected with forward and side scatter gated for lymphocytes. The expression of CD49b and tumor necrosis factor-related apoptosis-inducing ligand (TRAIL) was analyzed in this population. **A**: Numbers in each histogram above the marker indicate the percentage of 'live'-gated cells deemed panCD49b+. **B**: CD49b and tumor necrosis factor-related apoptosis-inducing ligand (TRAIL) profile of cells recovered from the cervical lymph node of mice pretreated with chitin microparticles or PBS. Figure is representative of three experiments.

related apoptosis-inducing ligand (TRAIL)-expressing natural killer cells increased 26-fold in the cervical lymph node of chitin microparticles treated mice compared with PBS-treated mice (Fig. 4B). These results suggest that migration of natural killer cells expressing tumor necrosis factor-related apoptosis-inducing ligand (TRAIL) into local lymph nodes might play a role in the reduction of virus titer and improvement of clinical symptoms in virus infected mice.

Reduction of IL-6 and Interferon-Gamma-Inducible Protein-10 (IP-10) Secretion From Nasal Mucosa by Pretreatment with Chitin Microparticles in H5N1 Influenza Virus Infection

Chitin microparticles might also play a role in the reduction of inflammatory cytokines and chemokines that accompany H5N1 influenza virus infection. To examine this possibility, the level of secreted cytokines described in the Materials and Methods in nasal mucosa was examined in mice infected with H5N1 virus with or without chitin microparticles pretreatment. Among them the secretion of IL-6 in nasal mucosa was up-regulated by H5N1 influenza virus infection 10 days post-inoculation, while in the chitin microparticles-treated group, there was a marked reduction of IL-6 secretion (Fig. 5A). Likewise, the secretion of interferon-gamma-inducible protein-10 (IP-10) was inhibited in mice pretreated with chitin microparticles compared to the PBS-treated group 8 days post-inoculation (Fig. 5B). On the other hand tumor necrosis factor-α was not detected in nasal mucosa of mice after H5N1 influenza virus infection (data not shown). These results suggested that chitin microparticles pretreatment may inhibit the hyper-induction induction of cytokines and chemokines that are relevant to the pathogenesis of H5N1 influenza virus in infected mice.

DISCUSSION

The present study demonstrated that intranasal administration of a suspension of chitin microparticles

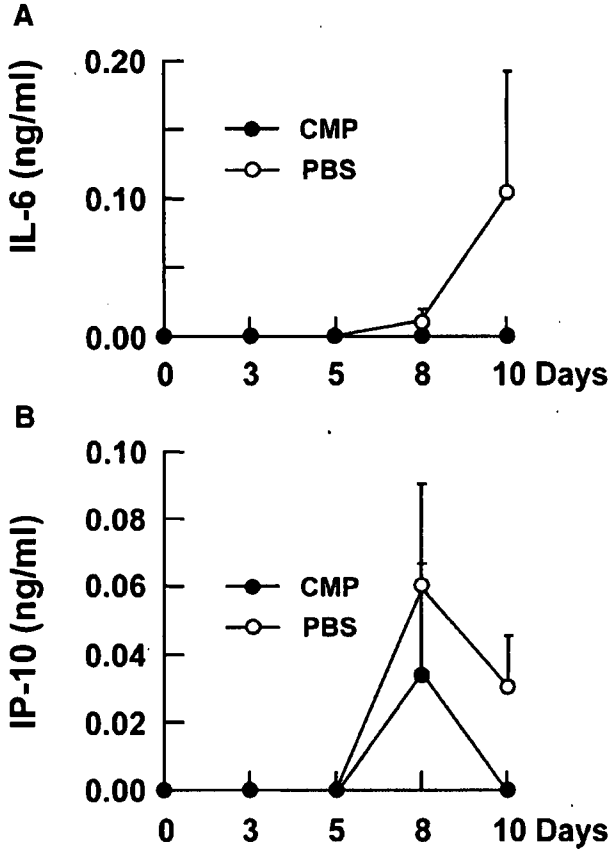

Fig. 5. Kinetics of IL-6 (A) and interferon-gamma-inducible protein-10 (IP-10) (B) secretion in the nasal mucosa after H5N1 influenza virus infection. Mice (n = 3) were administered 100 μg of chitin microparticles (CMP) intranasally once a day for 2 days (closed circles) or PBS (open circles), then infected with 1,000 PFU of VN1194 (H5N1) influenza virus. After viral challenge, mice were sacrificed to collect nasal washes 3, 5, 8, or 10 days post-inoculation. The levels of each cytokine in nasal washes after the viral challenge are shown. Data represents the means ± SE.

has protective effects against lethal H5N1 influenza virus infection of the upper respiratory tract in mice. These findings were consistent with results showing the protective effects against avirulent influenza virus (A/PR8, H1N1) infection in mice by intranasal administration of chitin microparticles into the lung (unpublished data by P. Strong). It is previously reported that chitin microparticles had a mucosal adjuvant effect when co-administered with an influenza hemagglutinin vaccine and increased both the mucosal and systemic humoral responses that provided complete protection against challenge with the homologous influenza virus H1N1 or H5N1 in mice [Hasegawa et al., 2005; Asahi-Ozaki et al., 2006; Ichinohe et al., 2006]. The current study demonstrates hitherto unrecognized effects of chitin microparticles in enhancing innate protection against infection with a highly pathogenic avian influenza virus strain.

It has been reported that the highly pathogenic H5N1 influenza virus induces high levels of pro-inflammatory cytokines and chemokines that may play a role in the pathogenesis of [Chan et al., 2005; de Jong et al., 2006]. It is demonstrated that intranasal administration of chitin microparticles induced the accumulation of natural killer cells expressing tumor necrosis factor-related apoptosis-inducing ligand (TRAIL) in the cervical lymph node and suppressed viral load and hyper-induction of cytokines. These results suggested that recruitment of natural killer cells expressing tumor necrosis factor-related apoptosis-inducing ligand (TRAIL) into local sites of infection (Fig. 4) and suppression of pro-inflammatory cytokines and chemokines (e.g. IL-6 and interferon-gamma-inducible protein-10 in Fig. 5) may contribute to a reduction of clinical symptoms and enhance protection against lethal H5N1 influenza virus infection.

The importance of natural killer cells in viral defense has been demonstrated most convincingly in a patient who lacked natural killer cells and was therefore susceptible to virus infections [Biron et al., 1989]. Mice in which natural killer cells have been depleted demonstrated increased mortality after infection with influenza viruses [Stein-Streilein and Guffee, 1986]. Therefore, it might be expected that the enhancement of natural killer cells activity by chitin microparticles and the accumulation of natural killer cells locally into the site of infection and an enhancement of tumor necrosis factor-related apoptosis-inducing ligand (TRAIL) expression on their surface (Fig. 4) might increase resistance to viral infection. In natural killer cells or T-cells, tumor necrosis factor-related apoptosis-inducing ligand (TRAIL) plays an important role in the immune response to influenza virus infection [Ishikawa et al., 2005]. Presumably due to this recruitment of tumor necrosis factor-related apoptosis-inducing ligand (TRAIL)-expressing natural killer cells, H5N1 virus titers were suppressed in nasal washes, lung washes, cervical lymph node, trigeminal nerve ganglia and in the brain stem of mice pretreated with chitin microparticles compared to mice in the control group (Fig. 3). Consistent with these findings, pretreatment of mice with chitin microparticles led to a significant improvement in survival rate and reduction in clinical symptoms following H5N1 virus infection (Fig. 2A,B) and H1N1 virus infection (Fig. 2C).

Finally, the present studies suggest that intranasal administration of chitin microparticles boosts innate immunity and protects mice from infection by the highly pathogenic H5N1 influenza virus infection in the upper respiratory tracts. It is proposed that if mice are given chitin microparticles as a daily prophylactic they would have enhanced protection against infection with H5N1. This prophylactic effect is elicited by activation of natural killer cells and regulation of inflammatory cytokines such as IL-6 and interferon-gamma-inducible protein-10 (IP-10). The adjuvant effects of chitin microparticles are also expected [Hasegawa et al., 2005; Asahi-Ozaki et al., 2006; Ichinohe et al., 2006] in inducing adaptive immunity following infection. Identification of therapeutic innate immunity enhancing agents such as chitin microparticles may lead to

antiviral strategies against the highly pathogenic H5N1 influenza virus and may have relevance as part of a first line defense against H5N1 outbreaks.

ACKNOWLEDGMENTS

We are grateful to Dr. Wilina Lim (Department of Health, The government of Hong Kong) for providing us A/Vietnam/1194/04 (H5N1) influenza virus strain, and Dr. U. Suzuki and Dr. K. Komase (Kitasato Institute, Saitama) and Dr. T. Tanaka (Toray Industries, Inc.) for providing the materials and Dr. M. Moriyama for helpful discussion. This work was supported in part by grants from the Ministry of Health, Labor, and Welfare, and Research on Health Sciences focusing on Drug Innovation.

REFERENCES

Andoniou CE, van Dommelen SL, Voigt V, Andrews DM, Brizard G, Asselin-Paturel C, Delale T, Stacey KJ, Trinchieri G, Degli-Esposti MA. 2005. Interaction between conventional dendritic cells and natural killer cells is integral to the activation of effective antiviral immunity. Nat Immunol 6:1011–1019.

Asahi Y, Yoshikawa T, Watanabe I, Iwasaki T, Hasegawa H, Sato Y, Shimada S, Nanno M, Matsuoka Y, Ohwaki M, Iwakura Y, Suzuki Y, Aizawa C, Sata T, Kurata T, Tamura S. 2002. Protection against influenza virus infection in polymeric Ig receptor knockout mice immunized intranasally with adjuvant-combined vaccines. J Immunol 168:2930–2938.

Asahi-Ozaki Y, Itamura S, Ichinohe T, Strong P, Tamura S, Takahashi H, Sawa H, Moriyama M, Tashiro M, Sata T, Kurata T, Hasegawa H. 2006. Intranasal administration of adjuvant-combined recombinant influenza virus HA vaccine protects mice from the lethal H5N1 virus infection. Microbes Infect 8:2706–2714.

Bacon A, Makin J, Sizer PJ, Jabbal-Gill I, Hinchcliffe M, Illum L, Chatfield S, Roberts M. 2000. Carbohydrate biopolymers enhance antibody responses to mucosally delivered vaccine antigens. Infect Immun 68:5764–5770.

Biron CA. 1997. Activation and function of natural killer cell responses during viral infections. Curr Opin Immunol 9:24–34.

Biron CA, Brossay L. 2001. NK cells and NKT cells in innate defense against viral infections. Curr Opin Immunol 13:458–464.

Biron CA, Byron KS, Sullivan JL. 1989. Severe herpesvirus infections in an adolescent without natural killer cells. N Engl J Med 320: 1731–1735.

Biron CA, Nguyen KB, Pien GC, Cousens LP, Salazar-Mather TP. 1999. Natural killer cells in antiviral defense: function and regulation by innate cytokines. Annu Rev Immunol 17:189–220.

Chan MC, Cheung CY, Chui WH, Tsao SW, Nicholls JM, Chan YO, Chan RW, Long HT, Poon LL, Guan Y, Peiris JS. 2005. Proinflammatory cytokine responses induced by influenza A (H5N1) viruses in primary human alveolar and bronchial epithelial cells. Respir Res 6:135.

Claas EC, Osterhaus AD, van Beek R, De Jong JC, Rimmelzwaan GF, Senne DA, Krauss S, Shortridge KF, Webster RG. 1998. Human influenza A H5N1 virus related to a highly pathogenic avian influenza virus. Lancet 351:472–477.

Cooper MA, Fehniger TA, Caligiuri MA. 2001. The biology of human natural killer-cell subsets. Trends Immunol 22:633–640.

de Jong MD, Simmons CP, Thanh TT, Hien VM, Smith GJ, Chau TN, Hoang DM, Van Vinh Chau N, Khanh TH, Dong VC, Qui PT, Van Cam B, Ha do Q, Guan Y, Peiris JS, Chinh NT, Hien TT, Farrar J. 2006. Fatal outcome of human influenza A (H5N1) is associated with high viral load and hypercytokinemia. Nat Med 12:1203–1207.

Gazit R, Gruda R, Elboim M, Arnon TI, Katz G, Achdout H, Hanna J, Qimron U, Landau G, Greenbaum E, Zakay-Rones Z, Porgador A, Mandelboim O. 2006. Lethal influenza infection in the absence of the natural killer cell receptor gene Ncr1. Nat Immunol 7:517–523.

Grose C, Chokephaibulkit K. 2004. Avian influenza virus infection of children in Vietnam and Thailand. Pediatr Infect Dis J 23: 793–794.

Hamajima K, Kojima Y, Matsui K, Toda Y, Jounai N, Ozaki T, Xin KQ, Strong P, Okuda K. 2003. Chitin micro-particles (CMP): a useful adjuvant for inducing viral specific immunity when delivered intranasally with an HIV-DNA vaccine. Viral Immunol 16:541–547.

Hasegawa H, Ichinohe T, Strong P, Watanabe I, Ito S, Tamura S, Takahashi H, Sawa H, Chiba J, Kurata T, Sata T. 2005. Protection against influenza virus infection by intranasal administration of hemagglutinin vaccine with chitin microparticles as an adjuvant. J Med Virol 75:130–136.

Ichinohe T, Watanabe I, Ito S, Fujii H, Moriyama M, Tamura S, Takahashi H, Sawa H, Chiba J, Kurata T, Sata T, Hasegawa H. 2005. Synthetic double-stranded RNA poly(I:C) combined with mucosal vaccine protects against influenza virus infection. J Virol 79:2910–2919.

Ichinohe T, Watanabe I, Tao E, Ito S, Kawaguchi A, Tamura S, Takahashi H, Sawa H, Moriyama M, Chiba J, Komase K, Suzuki Y, Kurata T, Sata T, Hasegawa H. 2006. Protection against influenza virus infection by intranasal vaccine with surf clam microparticles (SMP) as an adjuvant. J Med Virol 78:954–963.

Ishikawa E, Nakazawa M, Yoshinari M, Minami M. 2005. Role of tumor necrosis factor-related apoptosis-inducing ligand in immune response to influenza virus infection in mice. J Virol 79:7658–7663.

Kos FJ, Engleman EG. 1996. Role of natural killer cells in the generation of influenza virus-specific cytotoxic T cells. Cell Immunol 173:1–6.

Le QM, Kiso M, Someya K, Sakai YT, Nguyen TH, Nguyen KH, Pham ND, Ngyen HH, Yamada S, Muramoto Y, Horimoto T, Takada A, Goto H, Suzuki T, Suzuki Y, Kawaoka Y. 2005. Avian flu: isolation of drug-resistant H5N1 virus. Nature 437:1108.

Okamoto Y, Minami S, Matsuhashi A, Sashiwa H, Saimoto H, Shigemasa Y, Tanigawa T, Tanaka Y, Tokura S. 1993. Application of polymeric *N*-acetyl-D-glucosamine (chitin) to veterinary practice. J Vet Med Sci 55:743–747.

O'Leary JG, Goodarzi M, Drayton DL, von Andrian UH. 2006. T cell- and B cell-independent adaptive immunity mediated by natural killer cells. Nat Immunol 7:507–516.

Ozdemir C, Yazi D, Aydogan M, Akkoc T, Bahceciler NN, Strong P, Barlan IB. 2006. Treatment with chitin microparticles is protective against lung histopathology in a murine asthma model. Clin Exp Allergy 36:960–968.

Peiris JS, Yu WC, Leung CW, Cheung CY, Ng WF, Nicholls JM, Ng TK, Chan KH, Lai ST, Lim WL, Yuen KY, Guan Y. 2004. Re-emergence of fatal human influenza A subtype H5N1 disease. Lancet 363:617–619.

Seo SH, Hoffmann E, Webster RG. 2002. Lethal H5N1 influenza viruses escape host anti-viral cytokine responses. Nat Med 8:950–954.

Shibata Y, Foster LA, Kurimoto M, Okamura H, Nakamura RM, Kawajiri K, Justice JP, Van Scott MR, Myrvik QN, Metzger WJ. 1998. Immunoregulatory roles of IL-10 in innate immunity: IL-10 inhibits macrophage production of IFN-gamma-inducing factors but enhances NK cell production of IFN-gamma. J Immunol 161:4283–4288.

Shibata Y, Foster LA, Metzger WJ, Myrvik QN. 1997a. Alveolar macrophage priming by intravenous administration of chitin particles, polymers of *N*-acetyl-D-glucosamine, in mice. Infect Immun 65:1734–1741.

Shibata Y, Metzger WJ, Myrvik QN. 1997b. Chitin particle-induced cell-mediated immunity is inhibited by soluble mannan: mannose receptor-mediated phagocytosis initiates IL-12 production. J Immunol 159:2462–2467.

Stein-Streilein J, Bennett M, Mann D, Kumar V. 1983. Natural killer cells in mouse lung: surface phenotype, target preference, and response to local influenza virus infection. J Immunol 131:2699–2704.

Stein-Streilein J, Guffee J. 1986. In vivo treatment of mice and hamsters with antibodies to asialo GM1 increases morbidity and mortality to pulmonary influenza infection. J Immunol 136:1435–1441.

Strong P, Clark H, Reid K. 2002. Intranasal application of chitin microparticles down-regulates symptoms of allergic hypersensitivity to *Dermatophagoides pteronyssinus* and *Aspergillus fumigatus* in murine models of allergy. Clin Exp Allergy 32:1794–1800.

Subbarao K, Klimov A, Katz J, Regnery H, Lim W, Hall H, Perdue M, Swayne D, Bender C, Huang J, Hemphill M, Rowe T, Shaw M, Xu X, Fukuda K, Cox N. 1998. Characterization of an avian influenza A

(H5N1) virus isolated from a child with a fatal respiratory illness. Science 279:393–396.

Tran TH, Nguyen TL, Nguyen TD, Luong TS, Pham PM, Nguyen VC, Pham TS, Vo CD, Le TQ, Ngo TT, Dao BK, Le PP, Nguyen TT, Hoang TL, Cao VT, Le TG, Nguyen DT, Le HN, Nguyen KT, Le HS, Le VT, Christiane D, Tran TT, Menno de J, Schultsz C, Cheng P, Lim W, Horby P, Farrar J. 2004. Avian influenza A (H5N1) in 10 patients in Vietnam. N Engl J Med 350:1179–1188.

World Health Organization. 2007. Cumulative number of confirmed human cases of avian influenza A/(H5N1) reported to WHO. http://www.who.int/csr/disease/avian_influenza/country/cases_table_2007_03_12/en/index.html